Chinese Journal of Natural Medicines

A comprehensive review on wedelolactone: natural sources, total synthesis, and pharmacological activities

Haiping Cai, Yue Wu, Xiaojin Zhang

Citation: Haiping Cai, Yue Wu, Xiaojin Zhang, A comprehensive review on wedelolactone: natural sources, total synthesis, and pharmacological activities, Chinese Journal of Natural Medicines, 2025, 23(2), 169−181. doi: 10.1016/S1875−5364(25)60821−1.

View online: https://doi.org/10.1016/S1875−5364(25)60821−1

Chinese Journal of Natural Medicines 23 (2025) 169-181

Contents lists available at ScienceDirect

Chinese Journal of Natural Medicines

journal homepage: www.cjnmcpu.com/

Review

A comprehensive review on wedelolactone: natural sources, total synthesis, and pharmacological activities

Haiping Cai, Yue Wu, Xiaojin Zhang*

State Key Laboratory of Natural Medicines, Jiangsu Key Laboratory of Drug Design and Optimization, and Department of Chemistry, China Pharmaceutical University, Nanjing 211198, China

ARTICLE INFO

Article history:
Received 8 July 2024
Revised 30 August 2024
Accepted 20 September 2024
Available online 20 February 2025

Keywords:
Natural product
Wedelolactone
Pharmacological activity
Synthesis
Mechanism

ABSTRACT

Plant-derived natural products have long been a vital source for developing therapeutic drugs. Wedelolactone (WDL), a coumestan isolated from *Eclipta prostrata*, *Wedelia calendulacea*, *Wedelia chinensis*, and *Sphagneticola trilobata*, demonstrates a broad spectrum of therapeutic potential, including anticancer, anti-inflammatory, anti-obesity, anti-myotoxic, antimicrobial, anti-diabetic, and tissue-protective activities. This review synthesizes information on the isolation, total synthesis, pharmacological activity, underlying mechanisms, and pharmacokinetic properties of WDL. Additionally, it offers insights into potential clinical applications and future drug discovery avenues utilizing WDL or its derivatives, either independently or in combination with other pharmaceuticals.

1. Introduction

Natural products serve as a vital source for novel drug design and development, owing to their diverse chemical structures and biological activities [1-4]. Notably, naturally occurring isoflavones, the most prevalent polyphenols in humans, offer health benefits through their antioxidant properties and possess significant potential for the development of medications targeting various diseases. Coumarins, a distinct subclass of isoflavones [5], are characterized by an oxygen-containing tetracyclic system. These compounds occur in both free states and as glycosides across numerous higher plants, originating as secondary metabolites [6]. Additionally, coumarins are present in certain microorganisms and animals [7].

Coumestans constitute a notable class of compounds derived from coumarin, characterized by both coumarin and benzofuran moieties. Prominent members of this family include cannabichromene, wedelolactone (WDL), and demethylwedelolactone, recognized as significant sources of phytoestrogens [8]. These compounds have attracted substantial research interest due to their potential as crucial chemical scaffolds for developing novel drug leads. Investigations have focused on their extraction, isolation, structural analysis, chemical synthesis, biological evaluation, and pharmacokinetics [9-11]. This review concentrates on WDL, summarizing current research on this natural product, its pharmacological effects, and underlying mechanisms. The objective is to provide a theoretical foundation for enhancing its bioavailability, clinical application, and potential drug combinations.

2. Sources and extraction methods of WDL

WDL is a coumestan compound extracted from plants in the Compositae family, including *Eclipta prostrata*, *Wedelia calendulacea*, *Wedelia chinensis,* and *Sphagneticola trilobata*. Its structure comprises three hydroxyl groups at the C-1, C-8, and C-9 and a methoxy group at the C-3 position. The primary source of WDL is the dried aerial part of *Eclipta prostrata*, a plant in the Asteraceae family. The systematic name of WDL is 1,8,9-trihydroxy-3-methoxy-6*H*-benzofuro[3,2-*c*]chromen-6-one. The core structure consists of a coumarin ring system, which includes a benzene ring and an *α*-pyrone ring connected by a shared carbon atom. A notable feature is the benzofuran ring, which forms a unique skeleton through cyclization, enhancing the molecular complexity. The unsaturated lactone ring enables interactions with biological macromolecules such as proteins. The hydroxyl (-OH) substituents at C-8 and C-9 positions are particularly significant, contributing to WDL's antioxidant and anti-inflammatory properties.

WDL, first extracted from *Wedelia calandulacea* in 1956 and subsequently isolated from *Eclipta alba* [12], presents significant challenges in its extraction from natural sources due to its low plant content and instability under alkaline conditions. Fig. 1 summarizes the commonly employed extraction and purification methods. As a polyphenol lactone and bioactive compound, WDL's scarcity and rapid degradation in alkaline environments complicate its isolation process. Multiple-column chromatography stands as the predominant technique for obtaining high-purity WDL, offering excellent selectivity and product purity. However, this method's limitations, including low output, reduced yield, extended production cycles, and high costs, impede its industrial-scale production.

* Corresponding author.
E-mail address: zxj@cpu.edu.cn

https://doi.org/10.1016/S1875-5364(25)60821-1

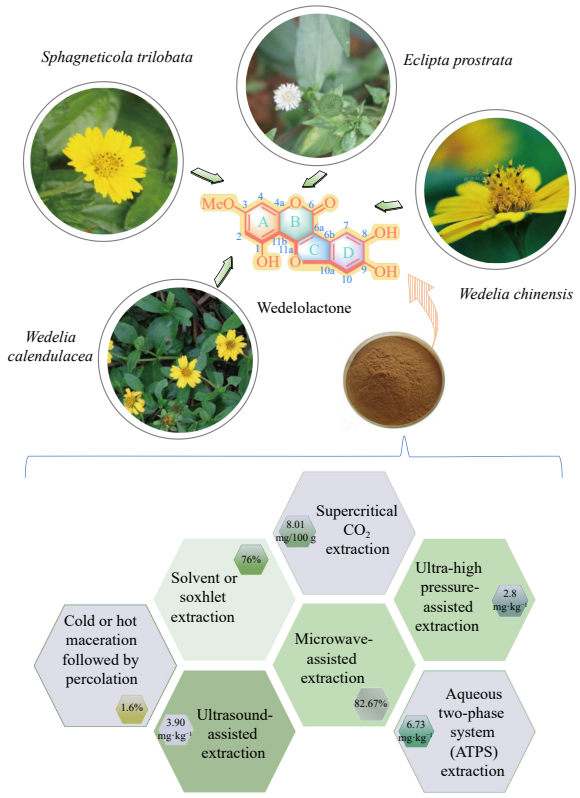

Fig. 1 Source and extraction method of wedelolactone (WDL). The above plant image elements are from the Chinese Field Herbarium (CFH).

2.1. Cold or hot maceration followed by percolation

The entire plant was air-dried and pulverized into coarse powder, then immersed in methanol for 24 h, percolated until colorless, and subsequently dried under vacuum at 40 °C to obtain WDL. The resulting dark green viscous substance was further dried under vacuum at 40 °C. To isolate WDL, this material was washed with toluene and fractionated using silica gel column chromatography. The yield of WDL extracted from *Eclipta alba* was 0.38% [13]. In an alternative approach, Unnikrishnan et al. utilized a reflux condenser with methanol to extract *E. alba* for 8–10 h, after which the extract was concentrated under vacuum at 40 °C using a rotary evaporator [14]. Jayathirtha et al. cleaned and dried *E. alba*, performed cold maceration with methanol, and then evaporated the solvent to dryness under vacuum. The concentration of WDL (1.6%) in the extracts was determined [15]. Diogo et al. extracted metabolites from pulverized and dried *E. alba* at room temperature using methanol and subsequently reconstituted the dried residue with methanol and water [16]. This method was considered the most conventional and straightforward to implement.

2.2. Solvent or soxhlet extraction

Shanshol et al. utilized a Soxhlet extractor to grind the dehydrated *Eclipta alba* plant into fine particles and subsequently extract them with anhydrous methanol at 50 °C for 36 h. The extract was then concentrated using a rotary evaporator and stored at 4 °C. The use of methanol as the extraction agent resulted in the highest yield, achieving 76% [17]. Patil et al. employed this technique to isolate WDL from *W. calendulacea* using methanol as the solvent, followed by evaporation and drying with a rotary evaporator [18]. While this purification method was effective, user-friendly, and required simple equipment, making it suitable for laboratory applications, it was time-intensive.

2.3. Ultrasound-assisted extraction

Fang et al. employed an ultrasound probe system (UPAE) to efficiently extract WDL from *Eclipta prostrata*. They optimized the extraction process utilizing a central composite design and response surface methodology (RSM). The identified optimal conditions comprised a 48% ethanol–water mixture, a temperature of 40 °C, an ultrasound power of 90 W, a solid-to-liquid ratio of 50 $mL \cdot g^{-1}$, and an extraction time of 11 min. This approach yielded 3.90 $mg \cdot g^{-1}$ of WDL, significantly reducing both extraction time and energy consumption [19]. While this method was energy-efficient and relatively environmentally friendly, it incurred high equipment costs and relied heavily on advanced technology.

2.4. Supercritical CO_2 extraction

Patil et al. utilized supercritical CO_2-assisted extraction (SC CO_2E) technology to isolate WDL from *Wedelia calendulacea*. The process involved compressing CO_2 from a cylinder to the desired working pressure using a cooling unit, followed by the introduction of methanol into the system *via* a solvent pump. The temperature and pressure of CO_2 were regulated to specific levels, and SC CO_2E was then allowed to contact the *W. calendulacea* powder thoroughly in the extractor. The resulting extract was collected, effectively yielding WDL. Under optimal extraction conditions, the process produced 8.01 mg/100 g of WDL [18]. While this method eliminated solvent residue and offered high purity and safety advantages, it was associated with high costs and technical complexity.

2.5. Microwave-assisted extraction

Shi et al. employed a round-bottom flask reflux system for WDL extraction from *Eclipta alba*. The process utilized 90% ethanol as the extraction solvent, applying 200 W microwave irradiation for 30 min. The extraction solution underwent concentration *via* rotary evaporation, followed by hot water filtration. The resulting aqueous solution was subjected to three ethyl acetate extractions. Subsequently, WDL was purified using a silica gel column. Under optimal conditions, the extraction rate of WDL reached 82.67%. The microwave-assisted extraction technique demonstrated advantages in WDL extraction, particularly in terms of efficiency and time [20]. This developed method proved to be environmentally friendly, rapid, cost-effective, and reliable, yielding higher extraction rates compared to alternative methods.

2.6. Ultra-high pressure-assisted extraction

This technique extracts WDL from Eclipta Herba by combining high-speed countercurrent chromatography with ultra-high pressure extraction. The crude powder of the medicinal material was sieved using a 60–80 mesh sieve, after which the extraction solvent was added to polyethylene bags and sealed and placed in an ultra-high pressure extraction vessel. Following centrifugation of the extract at 6000 $r \cdot min^{-1}$ for 5 min, it was filtered through a 0.45 μm filter. WDL was separated using a high-speed countercurrent chromatography system with a petroleum ether–ethyl acetate–methanol–water biphasic solvent system (3∶7∶5∶5). The WDL content was determined by high-performance liquid chromatography. The extraction efficiency of the method was 2.8 $mg \cdot g^{-1}$, comparable to that of heat reflux. Notably, the extraction time was significantly reduced from 60 to 3 min [21].

2.7. Aqueous two-phase system (ATPS) extraction

Gharat et al. developed an ATPS utilizing polyethylene glycol

(PEG) of varying molecular weights and sodium citrate to extract WDL from *Eclipta alba*. In this system, sodium citrate formed the bottom phase (salt) while PEG constituted the top phase (polymer). The mixture, adjusted to a specific pH, was combined with a measured amount of dry powder in a conical flask. It was then agitated for 2 h at 600 r·min^{-1} and subsequently centrifuged. The resulting mixture was separated using a separating funnel. High-performance liquid chromatography analysis demonstrated that the extraction efficiency of ATPS was 1.3 times higher than that of solvent or Soxhlet extraction. Under optimized conditions, the maximum extraction rate achieved was 6.73 mg·g^{-1} [22]. ATPS exhibited a higher extraction rate and operated under mild conditions, as WDL is rapidly transferred to the polymer phase after extraction from the bulk phase.

3. Total synthesis of WDL

Several methods for synthesizing WDL have been developed, primarily utilizing routes 1–5 as depicted in Fig. 2. Route 1 employed the Sonogashira reaction, involving the coupling of two key intermediates, followed by deprotection, reduction, and cyclization to yield WDL. However, this approach necessitated the preparation of a crucial intermediate phenylacetylene, which proved challenging. With an overall yield of 15%, this method was protracted and complicated the acquisition of various WDL analogs for structural modification [23]. Route 2 incorporated Pd-catalyzed cross-coupling, followed by cyclization, deprotection, methylation, and deprotection to obtain WDL. The utilization of toxic tin and mercury reagents impeded industrial production [24]. Route 3 encompassed C-C coupling, methylation, de-PMB protection, and debenzylation to produce WDL. Despite employing expensive catalysts, this method also involved a lengthy process and low yield [25]. Route 4 entailed heating phenylacetone to obtain 4,5-dihydroxy-7-methoxycoumarin, then utilizing an enzyme from sweet potato juice for dual cross-coupling with catechol to generate WDL. This approach significantly abbreviated the synthetic process, enabling the creation of numerous novel WDL analogs, which still require evaluation for biological effects [26]. Route 5 involved palladium-catalyzed Suzuki coupling and acid-promoted intramolecular transesterification, followed by deprotection and cyclization to afford WDL. With fewer synthetic steps and a higher yield, this method is more suitable for industrial production [27].

4. Pharmacological activities of WDL

WDL, a naturally occurring metabolite, is predominantly found in the genera *Eclipta* and *Wedelia*. Recent investigations have advanced our understanding of WDL's pharmacological properties. Studies conducted from 1956 to the present have elucidated its diverse therapeutic effects, encompassing anticancer, anti-inflammatory, anti-obesity, anti-myotoxic, antimicrobial, anti-diabetic, neuroprotective, cardioprotective, hepatoprotective, bone protective, dental protective, renal protective, lung protective, and eye-protective activities. WDL primarily exerts its biological effects through mechanisms associated with inflammation, oxidative stress, apoptosis, and hyperlipidemia. Table S1 provides a comprehensive summary of the pathways, potential targets, and indications of WDL related to its various activities [28-66]. Fig. 3 illustrates these associated regulatory factors.

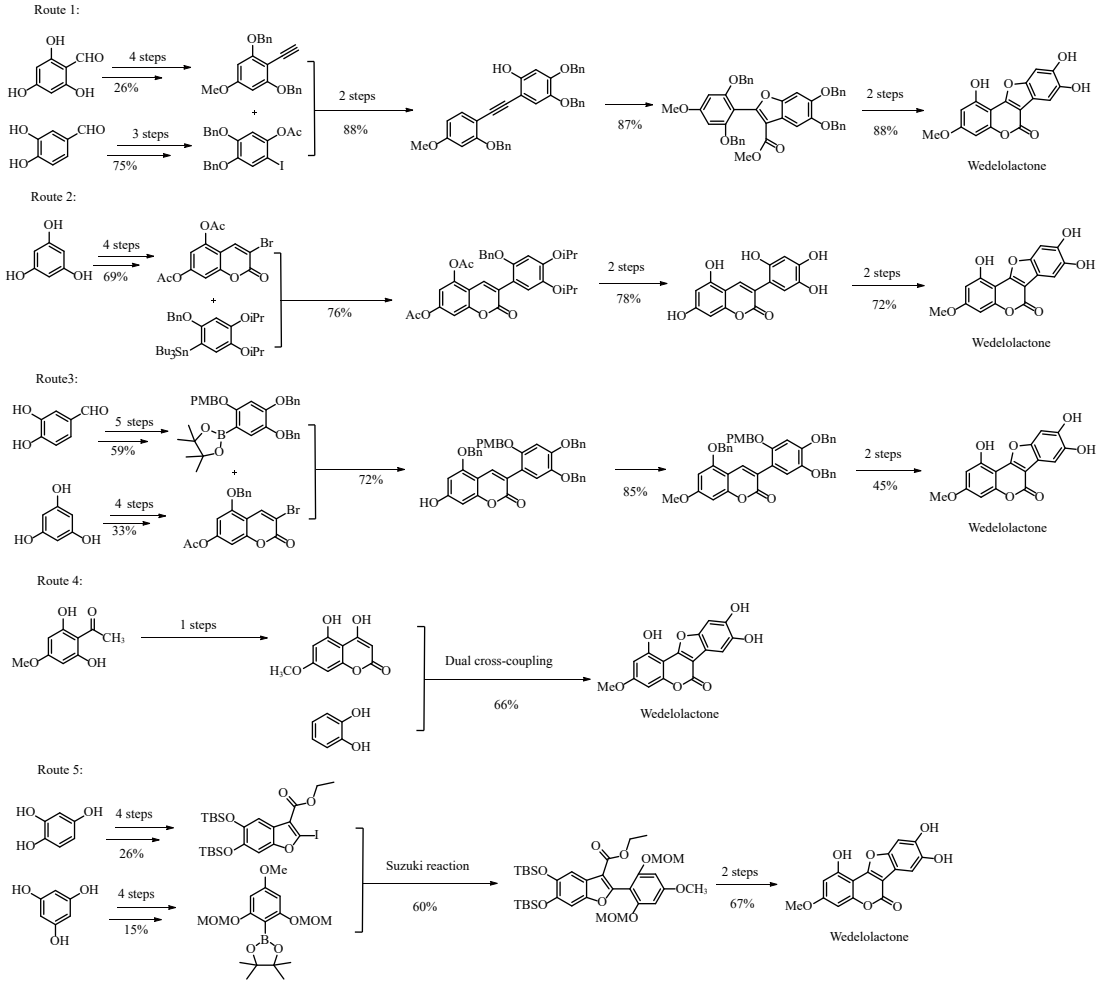

Fig. 2 Five routes for the total synthesis of wedelolactone.

4.1. Anticancer activity

The anticancer effects of WDL have been extensively studied, and the specific mechanisms involved are summarized in Fig. 4. Benesand et al. reported that WDL (10−30 μmol·L^{-1}) inhibits cancer cell growth by blocking the S and G_2/M phases of the cell cycle and inducing DNA damage signaling pathways, independent of nuclear factor-κB (NF-κB) and androgen receptors [67]. WDL interacts with double-stranded DNA and inhibits the activity of DNA topoisomerase IIα [28, 68]. Lee et al. demonstrated that WDL (20 μmol·L^{-1}) reduces matrix metalloproteinase (MMP) expression, which in turn blocks the IκB-α/NF-κB and MEK/ERK signaling pathways in MDA-MB-231 cancer cells, thereby inhibiting invasive growth [29, 69]. Sarveswaran et al. found that WDL (30 μmol·L^{-1}) induces caspase-dependent apoptosis in three prostate cancer cell lines (LNCaP, PC3, and DU145) by downregulating epsilon protein kinase C (PKCε), without inhibiting the Akt pathway [30, 70].

Nehybova's research demonstrated that WDL functions as a phytoestrogen in MDA-MB-231, MCF-7, and T47D breast cancer cells by activating both genomic and non-genomic estrogen receptor pathways at a low concentration of 10 nmol·L^{-1} [31, 71]. Furthermore, WDL inhibits proteasome activities (chymotrypsin-like, trypsin-like, and caspase-like) in breast cancer cells, exhibiting cytotoxicity towards these cells [72]. Sarveswaran et al. showed that WDL significantly downregulates c-Myc mRNA expression in prostate cancer cells and inhibits c-Myc protein levels, nuclear accumulation, DNA binding, and transcriptional activity [32]. Peng et al. reported that WDL (10−40 μmol·L^{-1}) inhibits melanoma cell proliferation and regulates the MV3 cell cycle by inhibiting Akt and activating MAPK pathways [73, 74], inducing the expression of pro-apoptotic proteins Bax and p21, while inhibiting anti-apoptotic proteins Bcl-2 and cyclin D [33].

Chen et al. demonstrated that WDL enhances the anticancer effects of IFN-γ in HepG2 cells by inhibiting TCPTP-mediated dephosphorylation of STAT1 at a concentration of 50 μmol·L^{-1} [34]. In another study, Chen et al. reported that WDL at 25 μmol·L^{-1} initiates a polycomb repressive complex 2 (PRC2)-dependent inhibition of cancer cell proliferation and induces cell cycle arrest and apoptosis by disrupting enhancer of zeste homolog 2 (EZH2)-EED interactions [35]. Romanchikova et al. found that WDL reduces MCL cell growth by modulating EZH2 and suppressing H3K27 methylation [36]. WDL can inhibit cancer progression by promoting apoptosis. Sarwar and colleagues investigated its effects on ovarian cancer cells and discovered that WDL induces apoptosis in MDA-MB-231 cancer cells by increasing Bax levels and decreasing Bcl-2 levels [75]. Additionally, PLGA-coated WDL nanoparticles at 10 μg·mL^{-1} enhance drug retention by inhibiting epithelial-mesenchymal transition (EMT) through the downregulation of sex-determining region Y-box 2 (SOX2) and ATP-binding cassette subfamily G member 2 (ABCG2) [76]. This process inhibits cell migration and invasion and reduces the percentage of breast cancer stem cells (BCSCs) in MDA-MB-231 cells [77].

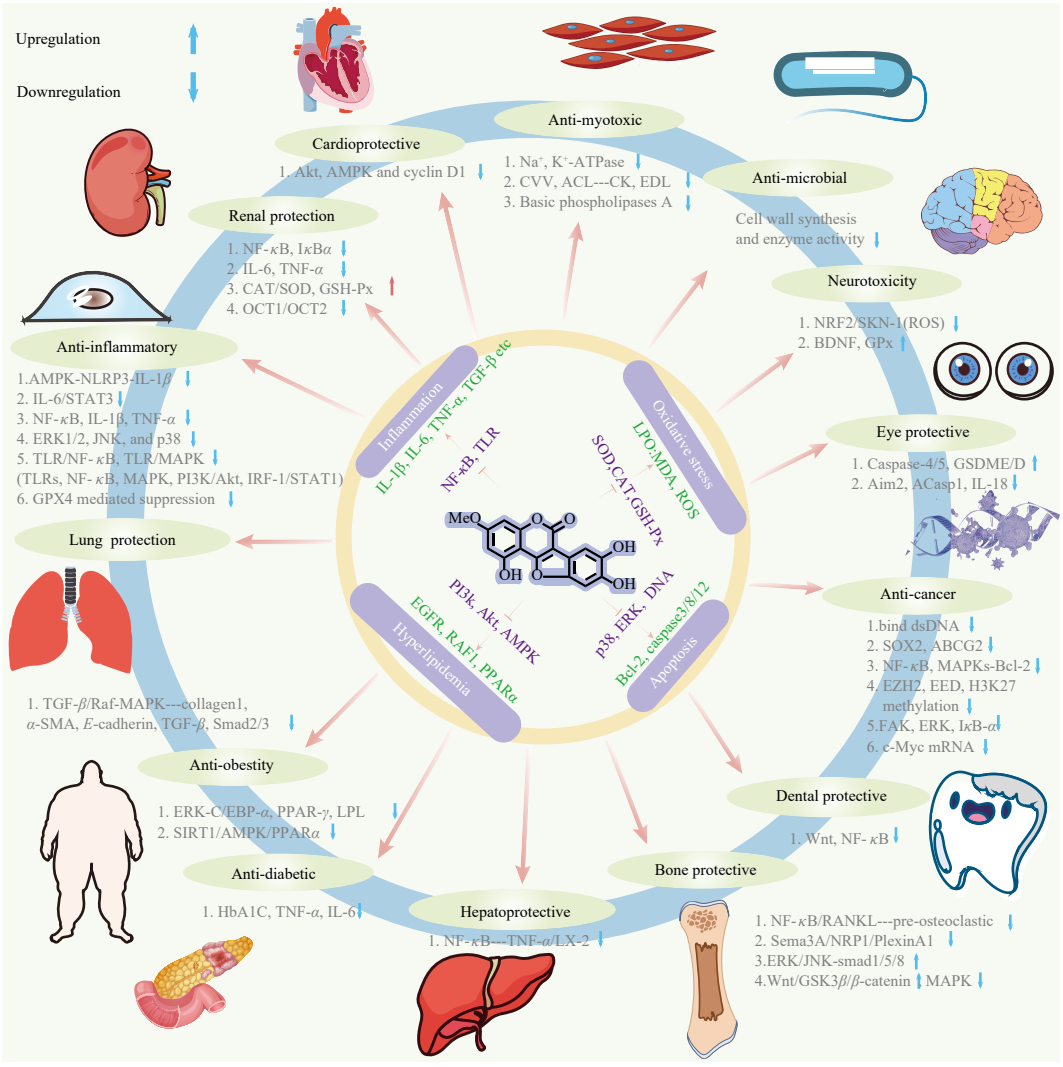

Fig. 3 Pharmacological activities of wedelolactone.

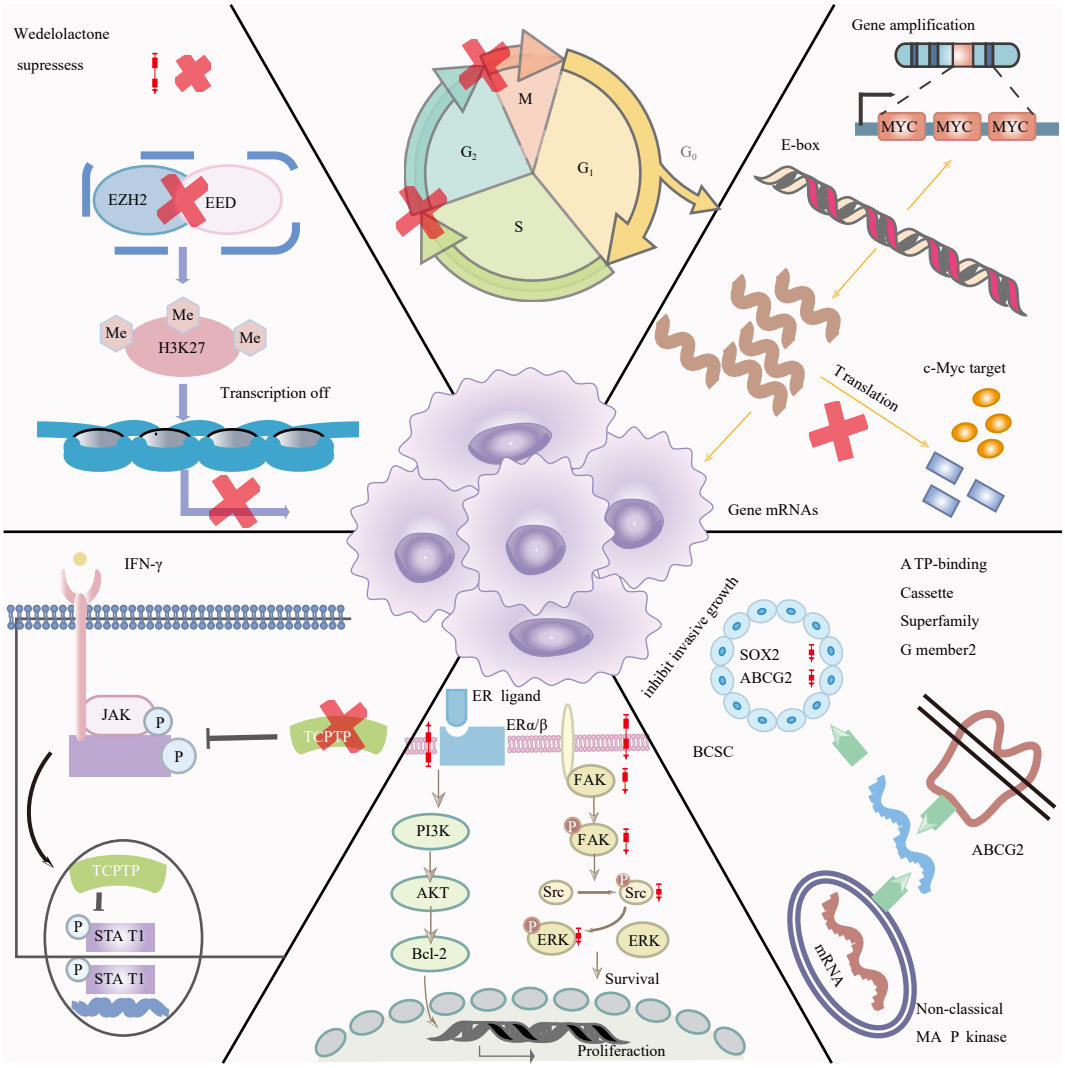

Fig. 4 Anticancer mechanism of wedelolactone.

4.2. Anti-inflammatory activity

The anti-inflammatory properties of WDL have been extensively studied, with the associated signaling pathways illustrated in Fig. 5. At a concentration of 100 μmol·L^{-1}, WDL inhibits lipopolysaccharide (LPS)-induced caspase-11 in BALB/c 3T3 cells through the NF-κB signaling pathway [37, 38, 78]. Similarly, WDL at 10 μmol·L^{-1} significantly reduces the levels of NO, prostaglandin E2 (PGE2), and tumor necrosis factor alpha (TNF-α), as well as the expression of inducible nitric oxide synthase (iNOS) and cyclooxygenase-2 (COX-2) in LPS-induced RAW 264.7 cells. This effect is achieved by degrading IκB-α and facilitating the translocation of the NF-κB p65 subunit [38, 79]. Moreover, WDL inhibits the activation of the NLR family pyrin domain containing 3 (NLRP3) inflammasome and the phosphorylation of caspase-1 *via* the AMPK-NLRP3-IL-1β axis, thereby reducing inflammation and potentially treating colitis [39, 80-83].

In bone marrow-derived macrophage (BMDM) cells, WDL (30 μg·mL^{-1}) effectively mitigates zymosan-induced inflammation by suppressing TNF-α, interleukin 6 (IL-6), IL-12p40, NADPH oxidase, and p47phox phosphorylation [40, 41, 84]. Furthermore, WDL (40 μmol·L^{-1}) enhances NLRP3 phosphorylation at the PKA-specific sites [85], activating the inflammasome and IL-1β secretion while attenuating monosodium urate (MSU)-induced inflammation and neutrophil migration, thus addressing gouty arthritis [41]. *In vivo* studies demonstrated that WDL (50 mg·kg^{-1}) exhibits anti-inflammatory effects in indomethacin-induced colitis by downregulating IL-6/STAT3 signaling and pro-inflammatory cytokines [42, 43, 86-89]. Additionally, in cases of acute pancreatitis, WDL at doses of 25 or 50 mg·kg^{-1} ameliorates the condition by upregulating glutathione peroxidase 4 (GPX4) expression and inhibiting both pyroptosis and ferroptosis [61]. These findings underscore the potential of WDL as a potent anti-inflammatory agent, which operates through multiple signaling pathways to exert its therapeutic effects. Soluble epoxide hydrolase (sEH) has been found to induce macrophage inactivation. WDL at concentrations of 5, 10, and 20 μmol·L^{-1} inhibits sEH activity, resulting in elevated levels of epoxyeicosatrienoic acids (EET). Consequently, this reduces inflammation and oxidative stress by modulating glycogen synthase kinase 3beta (GSK3β)-mediated NF-κB and nuclear factor E2-related factor 2 (Nrf2) pathways *in vitro* [44].

4.3. Anti-obesity activity

WDL shows promise in the treatment of obesity and associated metabolic disorders [90]. Initial investigations revealed that WDL inhibits adipogenesis-related proteins, including CCAAT/enhancer binding protein alpha (C/EBP-α), peroxisome proliferator-activated receptor gamma (PPAR-γ), and lipoprotein lipase (LPL) in hAMSCs *via* the ERK pathway [45]. Subsequent research demonstrated that WDL at concentrations of 5, 10, and 25 μmol·L^{-1} decreases lipid levels and ameliorates steatosis in HepG2 cells by activating AMPK pathways and upregulating PPARα/LPL and low-density lipoprotein receptor (LDLR) expres-

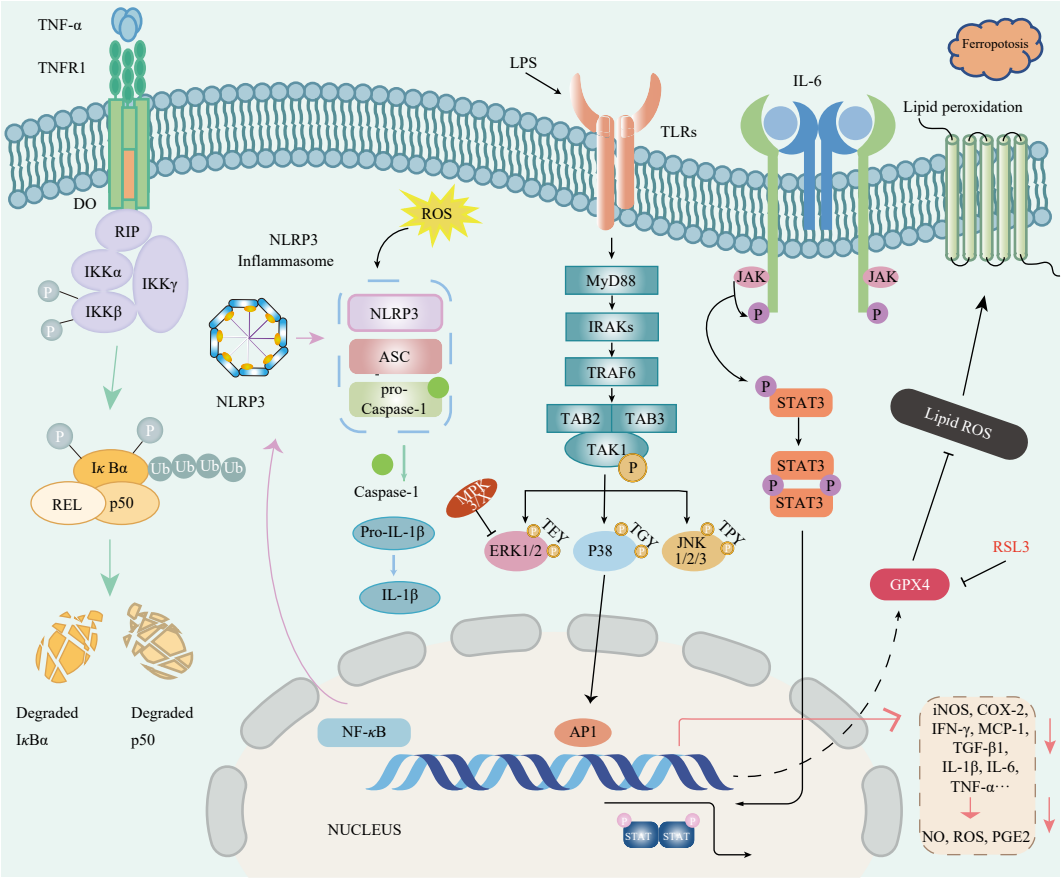

Fig. 5 Anti-inflammatory mechanism of wedelolactone.

sion [46, 91]. In high-fat diet (HFD)-induced hyperlipidemic hamsters, WDL administration at doses of 10, 20, and 40 mg·kg^{-1}·d^{-1} reduced lipid profiles, including TC, triglyceride (TG), and low-density lipoprotein cholesterol (LDL-C) *in vivo* [92-94]. Furthermore, WDL at 5 mg·kg^{-1}·d^{-1} decreased body weight in mice by inhibiting nicotinamide *N*-methyltransferase (NNMT) and stimulating fat browning through the sirtuin-1 (SIRT1)/AMPK/PPARα pathway [47].

4.4. Anti-myotoxic activity

Muscle toxins present in snake and lizard venom can induce rapid paralysis in prey. Research suggests that WDL may function as an effective antidote by inhibiting Na^+/K^+-ATPase activity with an IC_{50} value of 0.7 μmol·L^{-1} and flunitrazepam binding to rat brain synaptosomes with an IC_{50} value of 2.0 μmol·L^{-1} [95-97]. Furthermore, *Eclipta prostrate* extract (5 mg·mL^{-1}) demonstrates a dose-dependent anti-toxic activity against MPV venom [98]. Diogo et al. reported that WDL counteracts muscle toxicity induced by basic phospholipase A2 from *Crotalus durissus* terrificus (CB) and *Bothrops jararacussu* (Bth TX-I and II). In murine models, WDL (2.5 μg·g^{-1}, i.p.) attenuated the myotoxic effects of venoms from *Crotalus durissus* terrificus (CB) and Bth TX-I and II, as well as their respective phospholipase A2 toxins, CVV and ACL [16].

4.5. Antimicrobial activity

WDL demonstrates antimicrobial properties through its interactions with various enzymes and receptors [99]. Research indicates that WDL can mitigate atypical pyroptosis in corneal keratitis induced by *P. aeruginosa*. It suppresses caspase-4/5/11 expression in LPS-stimulated human corneal keratocytes, markedly alleviating inflammation and epithelial defects when used in conjunction with ciprofloxacin [63]. Furthermore, WDL inhibits neutrophil infiltration and decreases myeloperoxidase levels in *Aspergillus fumigatus*-induced fungal keratitis. It also reduces caspase-1 activity, resulting in lower IL-1β levels and a diminished host immune response [64]. Studies by Vinayagam et al. revealed that WDL targets bacterial nuclei and degrades bacterial cell walls, exhibiting efficacy against *E. coli*, *S. aureus*, *P. aeruginosa*, and *K. pneumoniae* [100, 101].

4.6. Anti-diabetic activity

WDL demonstrates efficacy as an anti-glycation agent both *in vivo* and *in vitro*, reducing glycated hemoglobin and fasting blood glucose levels. Kumar et al. reported that WDL inhibits *α*-glucosidase and *α*-amylase with inhibition rates of 80.65% and 93.83%, respectively [102-104]. Furthermore, WDL downregulated inflammatory mediators, including C-reactive protein (CRP), TNF-α, and IL-6 in mice at doses of 5, 10, and 20 mg·kg^{-1}. At a concentration of 30 μmol·L^{-1}, WDL reduced immune cell infiltration, inhibited hyperglycemia in zebrafish larvae, and protected human *β*-cells from cytokine-induced damage [105]. In di(2-ethylhexyl) phthalate (DEHP)-induced RIN-5F cells, WDL (80 μg·mL^{-1}) regulated Bcl-2 protein expression through the glucose transporter 2 (GLUT2) pathway, significantly enhancing antioxidant activity and insulin secretion [106].

4.7. Neuroprotective activity

Aluminum exposure can disrupt various ions, leading to excitotoxicity, oxidative stress, neuronal transport abnormalities, mitochondrial damage, apoptosis, inflammatory mediator release, and microglial activation. These effects contribute to numerous neurodegenerative disorders, including sporadic

amyotrophic lateral sclerosis (sALS). Fig. 6 illustrates how WDL modulates these ions to elicit neuroprotective effects [107, 108]. Administered at doses of 100 or 200 mg·kg^{-1}, WDL demonstrates neuroprotective properties by downregulating inflammatory cytokines such as TNF-α, IL-6, and IL-β [109]. It also enhances antioxidant levels and brain-derived neurotrophic factors, counteracting the detrimental effects of glutamate-induced excitotoxicity [110]. Furthermore, WDL increases BDNF and GPx expression to protect motor neurons from $AlCl_3$-induced toxicity while suppressing caspase-3 activation and inflammatory cytokines [111]. Post-therapy administration of WDL elevates vascular endothelial growth factor (VEGF), insulin-like growth factor-1 (IGF-1), and *N*-acetylaspartate (NAA) levels in the brain. Recent studies indicate that WDL mitigates Parkinson's disease by inhibiting various stress responses, including superoxide dismutase 5 (SOD-5), glutathione transferase-4 (GST-4), and skinhead-1 (SKN-1), as well as *α*-synuclein in the substantia nigra, and modifying mitochondrial genes (pink-1) [112].

4.8. Cardioprotective activity

Cardiovascular disease represents a significant, often underestimated threat among contemporary health issues [113-116]. WDL demonstrates substantial inhibitory effects on the proliferation of primary rat aortic vascular smooth muscle cells (VSMCs) at concentrations of 5–40 μmol·L^{-1}, induced by platelet-derived growth factor (PDGF). The underlying mechanism involves G_0/G_1 phase arrest, impeding cell cycle progression into the S phase, inhibiting Akt, and subsequently activating AMPK through the non-cyclin-dependent kinase inhibitor p21 [48]. Furthermore, WDL at 50 mg·kg^{-1} significantly reduces the neointima-to-media area ratio in balloon-injured rat carotid arteries. WDL also exhibits cardiovascular protective effects by ameliorating lipid abnormalities, such as reducing triglycerides (TG), very low-density lipoprotein cholesterol (VLDL-C), and TC, and by upregulating peroxisome proliferator-activated receptor alpha (PPAR-α) and activating the AMPK pathway [46, 117].

4.9. Hepatoprotective activity

Research indicates that WDL demonstrates antifibrotic effects on LX-2 hepatic stellate cells at concentrations ranging from 10–40 μmol·L^{-1}. Its mechanism involves reducing apoptotic Bcl-2 expression, enhancing ERK and JNK expression, and suppressing NF-*κ*B-mediated activity [118, 119]. In a CCl_4-induced mouse liver fibrosis model [120-122], intravenous administration of WDL (20 mg·kg^{-1}) combined with schisandrol B (40 mg·kg^{-1}) exhibits enhanced liver protection compared to individual treatments. This hepatoprotective effect is attributed to the modulation of transforming growth factor-β1 (TGF-β1) and NF-*κ*B signaling pathways [123-127]. Intragastric administration of WDL at 100 mg·kg^{-1} activates the farnesoid X receptor (FXR) *via* the FXR-bile acid-NF-*κ*B/NRF2 axis. This activation upregulates downstream BA transporter genes, including bile salt export pump (BSEP), ATP-binding cassette sub-family C member 2 (MRP2), and multidrug resistance protein 2 (MDR2). Consequently, this promotes BA efflux and inhibits inflammation and oxidative damage resulting from BA accumulation, thereby mitigating cholestatic liver injury [51].

4.10. Bone protective activity

Osteoporosis, a chronic metabolic bone disease, presents a significant health challenge [128]. Studies have shown that WDL primarily enhances osteoblast formation while inhibiting osteoclast proliferation and differentiation through two main pathways, as illustrated in Fig. 7. WDL upregulates the expression of osteoblast differentiation markers such as osteocalcin, runt-related transcription factor 2 (Runx2), and osterix, thereby suppressing osteoclast-mediated bone resorption [129, 130]. Moreover, at a concentration of 2 μg·mL^{-1}, WDL inhibits the RANKL/RANK/NF-*κ*B pathway, leading to the prevention of c-fos/cytoplasmic factor of activated T cell-1 (NFATc1) nuclear translocation [131-133]. As a result, WDL notably decreases the gene expression of osteoclastogenesis-related markers, including c-Src and cathepsin K (CTSK) [53, 134, 135]. The inhibition of osteoclastogenesis by WDL is likely attributed to increased expression and secretion of Sema3A and Sema7A in osteoblasts, activation of Sema3A/PlexinA1/Nrp1 and Sema7A-plexinc1-beta1 signaling, and subsequent inhibition of downstream phospholipase C gamma 2 (PLCγ2) in osteoclasts [52].

Additionally, WDL inhibits Akt activation while stimulating AMPK activation, effectively protecting mesenchymal stem cells from hydroxyl radical-induced oxidative stress. This protective effect suggests the potential use of WDL in mesenchymal stem cell transplantation for osteoporosis treatment. The mechanism involves free radical scavenging *via* electron transfer and radical adduct formation (RAF) pathways [129]. Moreover, WDL signaling through semaphorin 4D (Sema4D) inhibits Sema4D/Plexin-B1 formation [54]. Studies utilizing RAW 264.7 cells co-cultured with bone marrow stromal cells and treated with WDL demonstrated its ability to inhibit osteoclastogenesis while promoting osteoblastogenesis. Treatment with WDL (2 μg·mL^{-1}) also significantly reduces bone morphogenetic protein-2 gene expression and decreases Smad-1/5/8 phosphorylation levels [55].

4.11. Dental protective activity

Dental pulp stem cells (DPSCs) play a critical role in dentistry due to their inherent capacity to differentiate into odontoblasts,

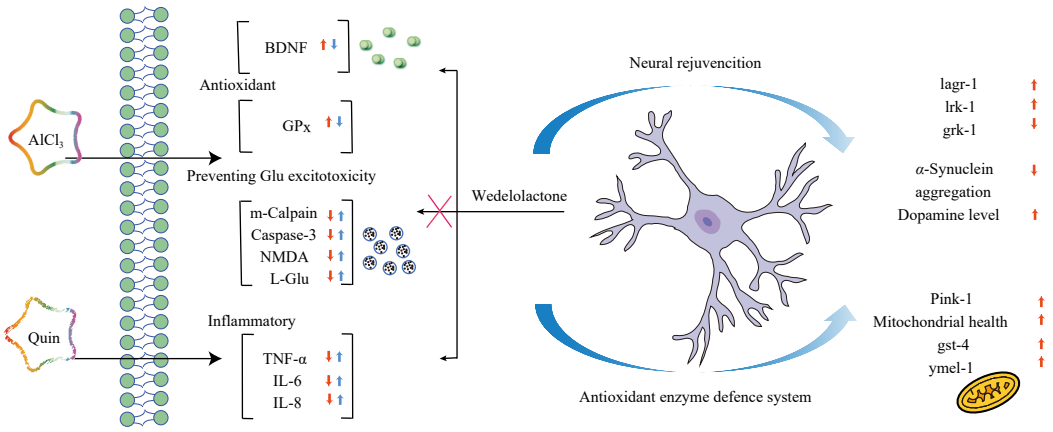

Fig. 6 Neuroprotective mechanism of wedelolactone.

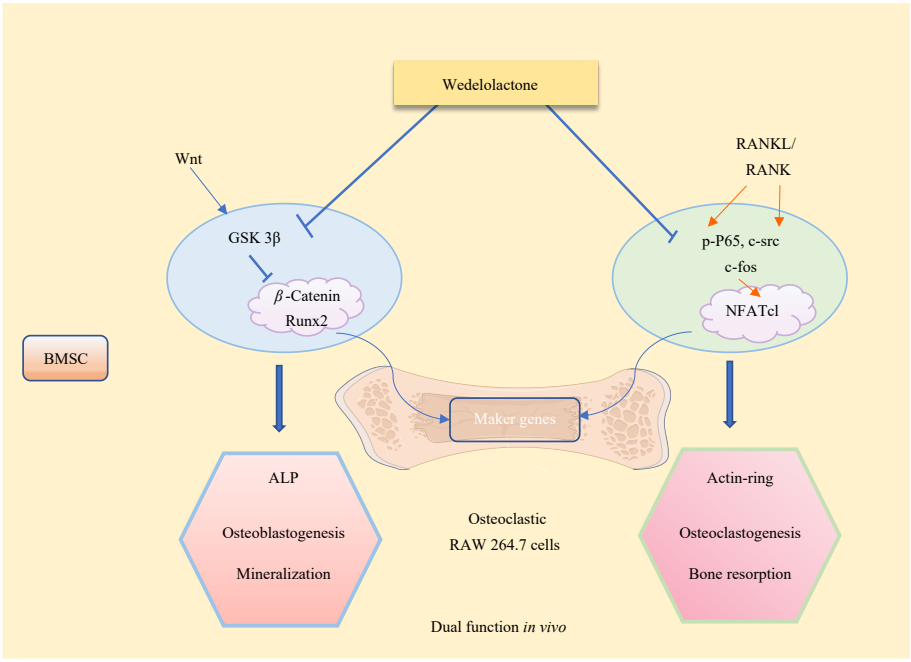

Fig. 7 Bone protective mechanism of wedelolactone.

which subsequently produce reparative dentin. WDL, at a concentration of 2 μg·mL^{-1}, enhances DPSC differentiation into odontoblasts by augmenting Wnt/*β*-catenin signaling and inhibiting NF-*κ*B. Post-odontoblastic differentiation, WDL activates *β*-catenin *via* the Sema3A/NRP1 (Sema3A/neuropilin-1) pathway, thereby stimulating the expression of marker genes dentin matrix protein-1 (DMP1), dentin sialophosphoprotein (DSPP), and Runx2. Furthermore, WDL upregulates I*κ*Bα expression, inhibits p65 phosphorylation, and prevents its nuclear translocation [136].

4.12. Renal protective activity

Numerous studies have elucidated the renal protective effects of WDL. Kidney injury, frequently associated with cytokine release by mesangial cells, may be attenuated by WDL. Research has demonstrated that WDL at concentrations of 10 and 20 μmol·L^{-1} inhibited the abnormal proliferation of human mesangial cells through the NF-*κ*B pathway [37, 56]. Furthermore, WDL mitigates renal toxicity, typically characterized by a rapid decline in kidney function due to exposure to drugs and toxins. Wang et al. showed that WDL alleviates cisplatin-induced toxicity in HEK293 cells by specifically inhibiting organic cation transporter 2 (OCT2) and nonspecifically inhibiting multidrug and toxin extrusion protein 1 (MATE1) [137-139]. WDL reduces inflammation markers such as IL-6, monocyte chemoattractant protein-1 (MCP-1), TNF-α, and TGF-β1 and regulates oxidative stress levels by increasing SOD, glutathione peroxidase (GSH-Px), and catalase (CAT) [57, 140, 141] dose-dependently at concentrations of 1.25, 5, and 20 μmol·L^{-1}. In nephrotoxic models, the combination of WDL with the NF-*κ*B inhibitor ammonium pyrrolidine dithiocarbamate (PDTC) decreased ROS and MDA levels in MPC-5 cells induced by doxorubicin through the IKK/I*κ*B/NF-*κ*B signaling pathway [57, 142]. At lower concentrations of 0.1, 1, and 10 μmol·L^{-1}, WDL ameliorated kidney injury by inhibiting inflammatory cytokines TNF-α, IL-1β, IL-6, and IL-8 and upregulating protein tyrosine phosphatase non-receptor type 2 (PTPN2) in HK-2 cells [143]. The mechanisms of WDL's renal protective effects are illustrated in Fig. 8.

4.13. Lung protective activity

WDL mitigates bleomycin-induced lung fibrosis syndrome in mice at a dose of 10 mg·kg^{-1} by activating AMPK and modulating the Raf-MAPKs signaling pathway [144, 145]. Furthermore, WDL (50 and 100 mg·kg^{-1}) ameliorates lung injury through GPX4-mediated mechanisms, thus reducing lung failure and ferroptosis [61]. WDL also exhibits potential against CCl_4-induced acute liver injury in mice by enhancing antioxidant capacity, suppressing inflammation, and decreasing apoptosis. The multiple mechanisms involve increased antioxidant enzymes such as SOD and GSH-Px, reduced expression of TNF-α, IL-1β, IL-6 mRNA, inhibition of ERK phosphorylation, and NF-*κ*B p65 translocation [146, 147], upregulated expression of c-Jun *N*-terminal kinase (JNK) and Bcl-2, and downregulated expression of Bax and caspase-3. Additionally, WDL inhibits TGF-β1-induced EMT and fibroblast differentiation by regulating both Smad and non-Smad signaling pathways [141, 148, 149], thereby improving pathological changes associated with lung fibrosis [60, 150, 151].

4.14. Eye protective activity

Retinal degenerative diseases, including retinitis pigmentosa, age-related macular degeneration, and retinal detachment, result in vision loss due to the degeneration of retinal photoreceptors [152]. Notably, the administration of WDL (1 μL, 200 μmol·L^{-1}) effectively mitigated retinal neurodegeneration caused by *N*-methyl-*N*-nitrosourea (NMU) in C57BL/6J mice by inhibiting the absence in melanoma 2 (AIM2)/caspase-11 pathway [62, 153]. Research has shown that WDL at concentrations of 10, 25, and 50 μmol·L^{-1} induces apoptosis and pyroptosis by elevating levels of mitochondrial ROS, caspase-3, caspase-1, gasdermin E (GSDME), and gasdermin D (GSDMD) activities. Furthermore, WDL enhances the condition of human corneal epithelial cells at concentrations of 1, 2, and 4 μmol·L^{-1}. It alleviates inflammation and corneal damage caused by *P. aeruginosa* by reducing caspase-4/5/11/GSDMD-mediated atypical pyroptosis [63]. In *Aspergillus fumigatus* keratitis infection models, WDL (10 μmol·L^{-1}) decreases neutrophil infiltration and IL-1β maturation in THP-1 macrophages and preserves corneal transparency *in vivo* [64].

4.15. Other activities

WDL demonstrates antiviral properties by inhibiting immedi-

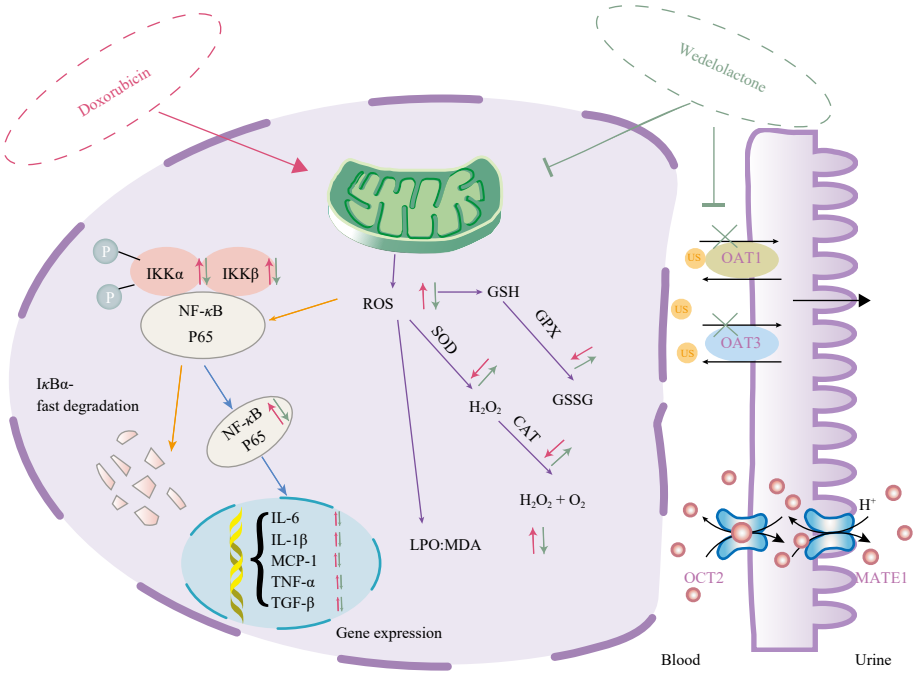

Fig. 8 Renal protective mechanism of wedelolactone.

ate-early protein 13/immediate-early protein 24 expression during human cytomegalovirus replication, thereby impeding viral replication. It interferes with the interaction between the EZH2 and components of the PRC2. This interference destabilizes PRC2 and related complexes, ultimately inhibiting viral replication [65, 154]. Li et al. reported that WDL enhances the viability of hydroxyl-treated mesenchymal stem cells primarily through its antioxidant activity, which involves single electron transfer, direct scavenging and inhibition of hydroxyl radicals and superoxide anions, and formation of radical adducts (e.g., reducing Cu^{2+} and chelating Fe^{2+}) [155]. WDL shows potential as an immunopotentiator. At a concentration of 100 μmol·L^{-1}, WDL upregulates the expression of perforin and granzyme B through the JAK/STAT signaling pathway, thereby enhancing the cytotoxic activity of natural killer cells (NK92-MI). Furthermore, WDL promotes the migration of NK-92MI cells by increasing the expression of CCR7 and CXCR4 in these cells [66, 156-159].

Despite its diverse range of activities, WDL demonstrates underlying commonalities primarily related to its interaction with key signaling pathways and its ability to modulate oxidative stress and inflammation. Specifically, the broad-spectrum activity of WDL is largely mediated through four major pathways: antioxidation, anti-inflammation, apoptosis, and hyperlipidemia. Furthermore, as a phytoestrogen, WDL activates both genomic and non-genomic signaling pathways, contributing to its effect on cancer treatment. Among these pathways, the inhibition of NF-κB is the most extensively studied. NF-κB plays a crucial role not only in anti-inflammatory activity but also in influencing the production of inflammatory mediators critical for organ protection. Additionally, WDL affects inflammation, blood pressure regulation, and neurotransmission by inhibiting enzymes associated with these physiological functions. These interactions highlight WDL's ability to regulate key enzymes and signaling pathways. Understanding these commonalities is essential for optimizing the therapeutic applications of WDL and for the development of novel drugs based on this natural product.

5. Pharmacokinetic properties of WDL

Initial pharmacokinetic studies on WDL utilized basic extracts from Eplica. Early research indicated that 10 mg of WDL in 10 mL of solution exhibited poor or partial solubility in both water and chloroform [160], with a water solubility of 0.5 mg·mL^{-1}, suggesting low solubility in both aqueous and lipid media [66]. Du et al. observed that when mice were orally administered a 70% ethanol extract from *E. prostrata* (8 g·kg^{-1}), WDL distributed across various organs within 8 min, with higher absorption in the liver and kidneys (> 200 ng·g^{-1}) [161]. Jiang et al. demonstrated that orally administered WDL (20 mg in MeOH) achieved a renal podocyte concentration of 0.057 mg·kg^{-1}, with a T_{max} of 1.5 h, a C_{max} of 6.39 μg·mL^{-1} and an AUC_{0-t} of 13.77 μg·h·L^{-1} using an HPLC-MS/MS method [162-168]. Cheruvu et al. reported that after oral administration of WDL (50 mg·kg^{-1}) in mice, the maximum plasma concentration (C_{max}) reached 4.4 ng·mL^{-1}, with a time-to-peak concentration (T_{max}) of 1 h and an area under the curve (AUC_{0-t}) of 27.5 ng·h·mL^{-1} [169]. Notably, they observed a second peak at 8 h, suggesting possible enterohepatic recirculation from bile reabsorption or reabsorption from distal parts of the small or large intestine into the bloodstream. Chen et al. reported that after oral administration of WDL (5.00 mg·kg^{-1}) to rats, the T_{max} was 0.5 h, the C_{max} was 15.22 mg·L^{-1}, and the $AUC_{0-\infty}$ was 83.05 mg·h·L^{-1} using a UPLC-MS/MS method [170-172]. Wang et al. found that after oral administration of WDL (0.1 mg·kg^{-1}) to rats, the T_{max} was 0.633 h, the C_{max} was 74.9 ng·mL^{-1}, and the AUC_{0-t} was 260.8 ng·h·mL^{-1} [173]. Further studies indicated that WDL undergoes extensive methylation, demethylation, glucuronidation, and hydrolysis after oral administration *in vivo*, resulting in relatively low oral bioavailability [174]. Current research focuses on improving its solubility and bioavailability through approaches such as WDL-loaded micelles [175], phyto-vesicles of WDL [160], ICG-liposomal WDL [176], and gold nanoshell coated WDL liposomes [177].

The pharmacokinetic parameters suggest that WDL is rapidly absorbed, achieving peak concentration shortly after oral administration. WDL demonstrates moderate absorption with significant tissue distribution, particularly in the kidneys. Its metabolism occurs primarily in the liver, generating various metabolites excreted through urine. The relatively short T_{max} and moderate C_{max} values indicate that frequent dosing may be required to maintain therapeutic levels, depending on the intended application. Moreover, WDL exhibits moderate oral bioavailability, potentially limited by its relatively low water solubility. To enhance its pharmacokinetic profile, strategies such as structural modific-

ation (e.g., methylation, acetylation) or the development of more soluble derivatives could be explored. Additionally, formulation approaches, including encapsulation in nanoparticles or liposomes, might improve its bioavailability and extend its half-life, potentially increasing its suitability for clinical use.

6. Conclusions

The direct isolation of the natural product WDL presents challenges due to its limited availability in nature, which impedes access to its active components for preclinical and clinical research and development. Moreover, industrial-scale production of the total synthetic route has not been established, further restricting its application. Additionally, the absence of systematic PK investigations on WDL hinders its clinical use, given its complex metabolic intricacies. There remains a significant gap in comprehensive studies on the safety profiles of WDL in humans and its effects on biological processes, genetics, protein interactions, and metabolism. Additional research is necessary to elucidate its PK properties, toxicity profiles, potential indications, and combination therapy strategies with other drugs. Developing high-yield methods, either chemical or biological, to obtain WDL and create structural derivatives is essential. Enhancing its solubility, bioavailability, and PK properties would establish a foundation for its clinical applications and drive its future development in pharmaceuticals, as well as in food and health products. The practical implications of WDL are considerable, given its potential as a natural therapeutic agent. Its capacity to modulate key biological pathways, such as NF-κB, AMPK, and Akt signaling, positions it as a promising natural product for the treatment of inflammatory and metabolic disorders. Furthermore, its role in reducing oxidative stress and enhancing immune responses suggests potential benefits in managing chronic diseases where inflammation and oxidative damage are key contributors. Future research can focus on several areas. First, efforts can be directed towards the synthesis of WDL derivatives to improve their bioavailability and metabolic stability through structural modification. Second, while preliminary studies have elucidated some molecular mechanisms underlying its pharmacological effects, more comprehensive research is required to fully elucidate its interactions with cell signaling pathways. This understanding will aid in identifying potential therapeutic targets, optimizing its application in specific clinical contexts, and uncovering possible drug interactions. Lastly, exploring the combined administration of WDL with other therapeutic agents and translating preclinical findings into practical applications are crucial for advancing its therapeutic potential.

Funding

This research was supported by the National Natural Science Foundation of China (No. 82322062) and Jiangsu Province Funds for Distinguished Young Scientists (No. BK20211527).

Declaration of competing interest

These authors have no conflict of interest to declare.

References

1 Davison EK, Brimble MA. Natural product derived privileged scaffolds in drug discovery. *Curr Opin Chem Biol*. 2019;52:1-8. https://doi.org/10.1016/j.cbpa.2018.12.007.
2 Yao H, Liu J, Xu S, et al. The structural modification of natural products for novel drug discovery. *Expert Opin Drug Discov*. 2017;12(2):121-140. https://doi.org/10.1080/17460441.2016.1272757.
3 Zhang NN, Jiang ZM, Li SZ, et al. Evolving interplay between natural products and gut microbiota. *Eur J Pharmacol*. 2023;949:175557. https://doi.org/10.1016/j.ejphar.2023.175557.
4 Luo Zw, Yin Fc, Wang Xb, et al. Progress in approved drugs from natural product resources. *Chin J Nat Med*. 2024;22(3):195-211. https://doi.org/10.1016/S1875-5364(24)60582-0.
5 Nehybová T, Šmarda J, Beneš P. Plant coumestans: recent advances and future perspectives in cancer therapy. *Anticancer Agents Med Chem*. 2014;14(10):1351-1362. https://doi.org/10.2174/1871520614666140713172949.
6 Soine TO. Naturally occurring coumarins and related physiological activities. *J Pharm Sci*. 1964;53:231-264. https://doi.org/10.1002/jps.2600530302.
7 Bourgaud F. Chemicals from plants. Perspectives on plant secondary products. *Plant Sci*. 2001;160(6):1249-1250. https://doi.org/10.1016/S0168-9452(01)00338-7.
8 Hwang KA, Choi KC. Anticarcinogenic effects of dietary phytoestrogens and their chemopreventive mechanisms. *Nutr Cancer*. 2015;67(5):796-803. https://doi.org/10.1080/01635581.2015.1040516.
9 Vinyagam R, Kumar P, Lee KE, et al. Biological and functional properties of wedelolactone in human chronic diseases. *Phyton-Int J Exp Bot*. 2021;90(1):1-15. https://doi.org/10.32604/phyton.2020.013388.
10 Tu Y, Yang Y, Li Y, et al. Naturally occurring coumestans from plants, their biological activities and therapeutic effects on human diseases. *Pharmacol Res*. 2021;169:105615. https://doi.org/10.1016/j.phrs.2021.105615.
11 Ha NM, Hop NQ, Son NT. Wedelolactone: a molecule of interests. *Fitoterapia*. 2023;164:105355. https://doi.org/10.1016/j.fitote.2022.105355.
12 Govindachari TR, Nagarajan K, Pai BR. Chemical examination of *Wedelia calendulacea*. Part I. Structure of wedelolactone. *J Chem Soc*. 1956(0):629-632. https://doi.org/10.1039/jr9560000629.
13 Kulkarni SR, Khatwani PF. Optimization of extraction conditions and development of a sensitive HPTLC method for estimation of wedelolactone in different extracts of *Eclipta alba*. *Int J Pharm Sci Drug Res*. 2011;3(1):56-61. https://doi.org/10.25004/IJPSDR.2011.030114.
14 Unnikrishnan KP, Fathima A, Hashim KM, et al. Antioxidant studies and determination of wedelolactone in *Eclipta alba*. *J Plant Sci*. 2007;2:459-464. https://doi.org/10.3923/jps.2007.459.464.
15 Jayathirtha MG, Mishra SH. Preliminary immunomodulatory activities of methanol extracts of *Eclipta alba* and *Centella asiatica*. *Phytomedicine*. 2004;11(4):361-365. https://doi.org/10.1078/0944711041495236.
16 Diogo LC, Fernandes RS, Marcussi S, et al. Inhibition of snake venoms and phospholipases A2 by extracts from native and genetically modified *Eclipta alba*: isolation of active coumestans. *Basic Clin Pharmacol Toxicol*. 2009;104(4):293-299. https://doi.org/10.1111/j.1742-7843.2008.00350.x.
17 Alaubydi M. The extraction and partial purification of wedelolactone from local *Eclipta alba* plant. *Iraqi J Sci*. 2013;54(4):1084-1089.
18 Patil AA, Sachin BS, Wakte PS, et al. Optimization of supercritical fluid extraction and HPLC identification of wedelolactone from *Wedelia calendulacea* by orthogonal array design. *J Adv Res*. 2014;5(6):629-635. https://doi.org/10.1016/j.jare.2013.09.002.
19 Fang X, Wang J, Wang Y, et al. Optimization of ultrasonic-assisted extraction of wedelolactone and antioxidant polyphenols from *Eclipta prostrate* L. using response surface methodology. *Sep Purif Technol*. 2014;138:55-64. https://doi.org/10.1016/j.seppur.2014.10.007.
20 Shi D, Ding H, Xu S. Optimization of microwave-assisted extraction of wedelolactone from *Eclipta alba* using response surface methodology. *Front Chem Sci Eng*. 2014;8(1):34-42. https://doi.org/10.1007/s11705-014-1401-6.
21 Zhao H, Cheng S, Zhang L, et al. Ultra-high-pressure-assisted extraction of wedelolactone and isodemethylwedelolactone from Ecliptae herba and purification by high-speed counter-current chromatography. *Biomed Chromatogr*. 2019;33(6):e4497. https://doi.org/10.1002/bmc.4497.
22 Gharat NN, Rathod VK. Response surface methodology for the extraction of wedelolactone from *Eclipta alba* using aqueous two-phase extraction. *Prep Biochem Biotechnol*. 2020;50(8):827-833. https://doi.org/10.1080/10826068.2020.1753071.
23 Li CC, Xie ZX, Zhang YD, et al. Total synthesis of wedelolactone. *J Org Chem*. 2003;68(22):8500-8504. https://doi.org/10.1021/jo030228f.
24 Chang CF, Yang LY, Chang SW, et al. Total synthesis of demethylwedelolactone and wedelolactone by Cu-mediated/Pd(0)-catalysis and oxidative-cyclization. *Tetrahedron*. 2008;64(17):3661-3666. https://doi.org/10.1016/j.tet.2008.02.031.
25 Huang H, Chen J, Ren J, et al. Palladium(II)-catalyzed efficient synthesis of wedelolactone and evaluation as potential tyrosinase inhibitor. *Molecules*. 2019;24(22):4130. https://doi.org/10.3390/molecules24224130.
26 Achari A, Chatterjee S, Dey S, et al. Catecholase-catalyzed synthesis of wedelolactone, a natural coumestan and its analogs. *Org Biomol Chem*. 2023;21(1):89-92. https://doi.org/10.1039/D2OB02081E.
27 Gou H, Zhang J, Li P, et al. A practical total synthesis of wedelolactone. *Synth Commun*. 2023;53(14):1126-1133. https://doi.org/10.1080/00397911.2023.2211772.
28 Benes P, Knopfova L, Trcka F, et al. Inhibition of topoisomerase IIα: novel function of wedelolactone. *Cancer Lett*. 2011;303(1):29-38. https://doi.org/10.1016/j.canlet.2011.01.002.
29 Lee YJ, Lin WL, Chen NF, et al. Demethylwedelolactone derivatives inhibit invasive growth *in vitro* and lung metastasis of MDA-MB-231 breast cancer cells in nude mice. *Eur J Med Chem*. 2012;56:361-367. https://doi.org/10.1016/j.ejmech.2012.07.041.
30 Sarveswaran S, Gautam SC, Ghosh J. Wedelolactone, a medicinal plant-derived coumestan, induces caspase-dependent apoptosis in prostate cancer cells *via* downregulation of PKCε without inhibiting Akt. *Int J Oncol*. 2012;41(6):2191-2199. https://doi.org/10.3892/ijo.2012.1664.
31 Nehybova T, Smarda J, Daniel L, et al. Wedelolactone induces growth of breast cancer cells by stimulation of estrogen receptor signalling. *J Steroid Biochem Mol Biol*. 2015;152:76-83. https://doi.org/10.1016/j.jsbmb.2015.04.019.
32 Sarveswaran S, Ghosh R, Parikh R, et al. Wedelolactone, an anti-inflammatory botanical, interrupts c-Myc oncogenic signaling and synergizes with enzalutamide to induce apoptosis in prostate cancer cells. *Mol Cancer Ther*. 2016;15(11):2791-2801. https://doi.org/10.1158/1535-7163.MCT-15-0861.
33 Peng YG, Zhang L. Wedelolactone suppresses cell proliferation and migration through AKT and AMPK signaling in melanoma. *J Dermatol Treat*.

2018;30(4):389-395. https://doi.org/10.1080/09546634.2018.1527996.
34 Chen Z, Sun X, Shen S, et al. Wedelolactone, a naturally occurring coumestan, enhances interferon-γ signaling through inhibiting STAT1 protein dephosphorylation. *J Biol Chem*. 2013;288(20):14417-14427. https://doi.org/10.1074/jbc.M112.442970.
35 Chen H, Gao S, Li J, et al. Wedelolactone disrupts the interaction of EZH2-EED complex and inhibits PRC2-dependent cancer. *Oncotarget*. 2015;6(15):13049-13059. https://doi.org/10.18632/oncotarget.3790.
36 Romanchikova N, Trapencieris P. Wedelolactone targets EZH2-mediated histone H3K27 methylation in mantle cell lymphoma. *Anticancer Res*. 2019;39(8):4179-4184. https://doi.org/10.21873/anticanres.13577.
37 Kobori M, Yang Z, Gong D, et al. Wedelolactone suppresses LPS-induced caspase-11 expression by directly inhibiting the IKK complex. *Cell Death Differ*. 2004;11(1):123-130. https://doi.org/10.1038/sj.cdd.4401325.
38 Yuan F, Chen J, Sun PP, et al. Wedelolactone inhibits LPS-induced pro-inflammation *via* NF-kappaB pathway in RAW 264.7 cells. *J Biomed Sci*. 2013;20(1):84. https://doi.org/10.1186/1423-0127-20-84.
39 Wei W, Ding M, Zhou K, et al. Protective effects of wedelolactone on dextran sodium sulfate induced murine colitis partly through inhibiting the NLRP3 inflammasome activation *via* AMPK signaling. *Biomed Pharmacother*. 2017;94:27-36. https://doi.org/10.1016/j.biopha.2017.06.071.
40 Cuong TT, Diem GH, Doan TT, et al. Wedelolactone from Vietnamese *Eclipta prostrata* (L) L. protected zymosan-induced shock in mice. *Iran J Pharm Res*. 2018;17(2):653-660.
41 Pan H, Lin Y, Dou J, et al. Wedelolactone facilitates Ser/Thr phosphorylation of NLRP3 dependent on PKA signalling to block inflammasome activation and pyroptosis. *Cell Prolif*. 2020;53(9):e12868. https://doi.org/10.1111/cpr.12868.
42 Tigari P, Janadri S, Madhu K, et al. Evaluation of anti-inflammatory effect of wedelolactone on indomethacin induced colitis in rats: involvement of IL-6/STAT3 pathway. *Biointerface Res Appl Chem*. 2021;12(3):2813-2825. https://doi.org/10.33263/BRIAC123.28132825.
43 Prakash T, Janadri S. Anti-inflammatory effect of wedelolactone on DSS induced colitis in rats: IL-6/STAT3 signaling pathway. *J Ayurveda Integr Med*. 2023;14(2):100544. https://doi.org/10.1016/j.jaim.2022.100544.
44 Zhang J, Zhang M, Huo XK, et al. Macrophage inactivation by small molecule wedelolactone *via* targeting sEH for the treatment of LPS-induced acute lung injury. *ACS Cent Sci*. 2023;9(3):440-456. https://doi.org/10.1021/acscentsci.2c01424.
45 Lim S, Jang HJ, Park EH, et al. Wedelolactone inhibits adipogenesis through the ERK pathway in human adipose tissue-derived mesenchymal stem cells. *J Cell Biochem*. 2012;113(11):3436-3445. https://doi.org/10.1002/jcb.24220.
46 Zhang Y, Zhao Y, Peng L, et al. Wedelolactone regulates lipid metabolism and improves hepatic steatosis partly by AMPK activation and up-regulation of expression of PPARα/LPL and LDLR. *PLoS One*. 2015;10(7):e0132720. https://doi.org/10.1371/journal.pone.0132720.
47 Yao E, Yang X, Huang X, et al. Phytochemical wedelolactone reverses obesity by prompting adipose browning through SIRT1/AMPK/PPARα pathway *via* targeting nicotinamide *N*-methyltransferase. *Phytomedicine*. 2022;94:153843. https://doi.org/10.1016/j.phymed.2021.153843.
48 Peng L, Huang X, Jin X, et al. Wedelolactone, a plant coumarin, prevents vascular smooth muscle cell proliferation and injury-induced neointimal hyperplasia through Akt and AMPK signaling. *Exp Gerontol*. 2017;96:73-81. https://doi.org/10.1016/j.exger.2017.06.011.
49 Luo Q, Ding J, Zhu L, et al. Hepatoprotective effect of wedelolactone against concanavalin a-induced liver injury in mice. *Am J Chin Med*. 2018;46(04):819-833. https://doi.org/10.1142/S0192415X1850043X.
50 Ai Y, Shi W, Zuo X, et al. The combination of schisandrol B and wedelolactone synergistically reverses hepatic fibrosis *via* modulating multiple signaling pathways in mice. *Front Pharmacol*. 2021;12:655531. https://doi.org/10.3389/fphar.2021.655531.
51 Wang MQ, Zhang KH, Liu FL, et al. Wedelolactone alleviates cholestatic liver injury by regulating FXR-bile acid-NF-κB/NRF2 axis to reduce bile acid accumulation and its subsequent inflammation and oxidative stress. *Phytomedicine*. 2024;122:155124. https://doi.org/10.1016/j.phymed.2023.155124.
52 Liu YQ, Han XF, Bo JX, et al. Wedelolactone enhances osteoblastogenesis but inhibits osteoclastogenesis through Sema3A/NRP1/PlexinA1 pathway. *Front Pharmacol*. 2016;7:375. https://doi.org/10.3389/fphar.2016.00375.
53 Liu YQ, Hong ZL, Zhan LB, et al. Wedelolactone enhances osteoblastogenesis by regulating Wnt/β-catenin signaling pathway but suppresses osteoclastogenesis by NF-κB/c-fos/NFATc1 pathway. *Sci Rep*. 2016;6(1):32260. https://doi.org/10.1038/srep32260.
54 Deng X, Liang LN, Zhu D, et al. Wedelolactone inhibits osteoclastogenesis but enhances osteoblastogenesis through altering different semaphorins production. *Int Immunopharmacol*. 2018;60:41-49. https://doi.org/10.1016/j.intimp.2018.04.037.
55 Zhu D, Deng X, Han XF, et al. Wedelolactone enhances osteoblastogenesis through ERK- and JNK-mediated BMP2 expression and Smad/1/5/8 phosphorylation. *Molecules*. 2018;23(3):561. https://doi.org/10.3390/molecules23030561.
56 Shen P, Yang X, Jiang J, et al. Wedelolactone from *Eclipta alba* inhibits lipopolysaccharide-enhanced cell proliferation of human renal mesangial cells *via* NF-κB signaling pathway. *Am J Transl Res*. 2017;9(5):2132-2142.
57 Zhu MM, Wang L, Yang D, et al. Wedelolactone alleviates doxorubicin-induced inflammation and oxidative stress damage of podocytes by IκK/IκB/NF-κB pathway. *Biomed Pharmacother*. 2019;117:109088. https://doi.org/10.1016/j.biopha.2019.109088.
58 Li C, Wang X, Bi Y, et al. Potent inhibitors of organic anion transporters 1 and 3 from natural compounds and their protective effect on aristolochic acid nephropathy. *Toxicol Sci*. 2020;175(2):279-291. https://doi.org/10.1093/toxsci/kfaa033.
59 Wang G, Bi Y, Xiong H, et al. Wedelolactone protects against cisplatin-induced nephrotoxicity in mice *via* inhibition of organic cation transporter 2. *Hum Exp Toxicol*. 2021;40(12_suppl):S447-S459. https://doi.org/10.1177/09603271211047915.
60 Yang JY, Tao LJ, Liu B, et al. Wedelolactone attenuates pulmonary fibrosis partly through activating AMPK and regulating Raf-MAPKs signaling pathway. *Front Pharmacol*. 2019;10:151. https://doi.org/10.3389/fphar.2019.00151.
61 Fan R, Sui J, Dong X, et al. Wedelolactone alleviates acute pancreatitis and associated lung injury *via* GPX4 mediated suppression of pyroptosis and ferroptosis. *Free Radic Biol Med*. 2021;173:29-40. https://doi.org/10.1016/j.freeradbiomed.2021.07.009.
62 Harkin K, Augustine J, Stitt AW, et al. Wedelolactone attenuates *N*-methyl-*N*-nitrosourea-induced retinal neurodegeneration through suppression of the AIM2/CASP11 pathway. *Biomedicines*. 2022;10(2):311. https://doi.org/10.3390/biomedicines10020311.
63 Xu S, Liu X, Liu X, et al. Wedelolactone ameliorates pseudomonas aeruginosa-induced inflammation and corneal injury by suppressing caspase-4/5/11/GSDMD-mediated non-canonical pyroptosis. *Exp Eye Res*. 2021;211:108750. https://doi.org/10.1016/j.exer.2021.108750.
64 Cheng M, Lin J, Li C, et al. Wedelolactone suppresses IL-1β maturation and neutrophil infiltration in aspergillus fumigatus keratitis. *Int Immunopharmacol*. 2019;73:17-22. https://doi.org/10.1016/j.intimp.2019.04.050.
65 Svrlanska A, Ruhland A, Marschall M, et al. Wedelolactone inhibits human cytomegalovirus replication by targeting distinct steps of the viral replication cycle. *Antiviral Res*. 2020;174:104677. https://doi.org/10.1016/j.antiviral.2019.104677.
66 Sun L, Sun W, Liu M, et al. Wedelolactone induces natural killer cell activity and the improvement to bioavailability using polysaccharides from ligustri lucidi fructus. *Int J Biol Macromol*. 2023;244:125208. https://doi.org/10.1016/j.ijbiomac.2023.125208.
67 Zhang M, Qu J, Gao Z, et al. Timosaponin aiii induces G_2/M arrest and apoptosis in breast cancer by activating the ATM/Chk2 and p38 MAPK signaling pathways. *Front Pharmacol*. 2021;11:601468. https://doi.org/10.3389/fphar.2020.601468.
68 Mi S, Liu X, Zhang L, et al. Chinese medicine formula 'Baipuhuang Keli' inhibits triple-negative breast cancer by hindering DNA damage repair *via* MAPK/ERK pathway. *J Ethnopharmacol*. 2023;304:116077. https://doi.org/10.1016/j.jep.2022.116077.
69 Dai Y, Zhou Q, Liu Y, et al. Ruscogenin alleviates deep venous thrombosis and pulmonary embolism induced by inferior vena cava stenosis inhibiting MEK/ERK/Egr-1/TF signaling pathway in mice. *Curr Pharm Des*. 2022;28(24):2001-2009. https://doi.org/10.2174/1381612828666220526120515.
70 Yang X, Gao M, Miao M, et al. Combining combretastatin A4 phosphate with ginsenoside Rd synergistically inhibited hepatocellular carcinoma by reducing HIF-1α *via* PI3K/AKT/mTOR signalling pathway. *J Pharm Pharmacol*. 2021;73(2):263-271. https://doi.org/10.1093/jpp/rgaa006.
71 Li Y, Hu Q, Li W, et al. Simultaneous blockage of contextual TGF-β by cyto-pharmaceuticals to suppress breast cancer metastasis. *J Control Release*. 2021;336:40-53. https://doi.org/10.1016/j.jconrel.2021.06.012.
72 Nehybová T, Šmarda J, Daniel L, et al. Wedelolactone acts as proteasome inhibitor in breast cancer cells. *Int J Mol Sci*. 2017;18(4):729. https://doi.org/10.3390/ijms18040729.
73 Yang Y, Zhou W, Xu X, et al. Aprepitant inhibits JNK and p38/MAPK to attenuate inflammation and suppresses inflammatory pain. *Front Pharmacol*. 2022;12:811584. https://doi.org/10.3389/fphar.2021.811584.
74 Xue C, Liu SX, Hu J, et al. *Corydalis saxicola* bunting total alkaloids attenuate paclitaxel-induced peripheral neuropathy through PKCε/p38 MAPK/TRPV1 signaling pathway. *Chin Med*. 2021;16(1):58. https://doi.org/10.1186/s13020-021-00468-5.
75 Sarwar S, Alamro AA, Alghamdi AA, et al. Enhanced accumulation of cisplatin in ovarian cancer cells from combination with wedelolactone and resulting inhibition of multiple epigenetic drivers. *Drug Des Devel Ther*. 2021;15:2211-2227. https://doi.org/10.2147/DDDT.S288707.
76 Zhang Y, Zhang M, Hu G, et al. Elevated system exposures of baicalin after combinatory oral administration of rhein and baicalin: mainly related to breast cancer resistance protein (ABCG2), not UDP-glucuronosyltransferases. *J Ethnopharmacol*. 2020;250:112528. https://doi.org/10.1016/j.jep.2019.112528.
77 Das S, Mukherjee P, Chatterjee R, et al. Enhancing chemosensitivity of breast cancer stem cells by downregulating SOX2 and ABCG2 using wedelolactone-encapsulated nanoparticles. *Mol Cancer Ther*. 2019;18(3):680-692. https://doi.org/10.1158/1535-7163.MCT-18-0409.
78 Liu JQ, Zhao M, Zhang Z, et al. Rg1 improves LPS-induced parkinsonian symptoms in mice *via* inhibition of NF-κB signaling and modulation of M1/M2 polarization. *Acta Pharmacol Sin*. 2020;41(4):523-534. https://doi.org/10.1038/s41401-020-0358-x.
79 Ou Y, Zhu L, Xu SY, et al. Activation of RAW264.7 macrophage by exopolysaccharide from aphanothece halaphytica (EPSAH) and the underlying mechanisms. *Fundam Clin Pharmacol*. 2020;34(5):591-602. https://doi.org/10.1111/fcp.12550.
80 Wang K, Lv Q, Miao YM, et al. Cardamonin, a natural flavone, alleviates inflammatory bowel disease by the inhibition of NLRP3 inflammasome activation *via* an ahr/Nrf2/nqo1 pathway. *Biochem Pharmacol*. 2018;155:494-509. https://doi.org/10.1016/j.bcp.2018.07.039.
81 Liang H, Cheng R, Wang J, et al. Mogrol, an aglycone of mogrosides, attenuates ulcerative colitis by promoting AMPK activation. *Phytomedicine*. 2021;81:153427. https://doi.org/10.1016/j.phymed.2020.153427.
82 Chai Y, Cai Y, Fu Y, et al. Salidroside ameliorates depression by suppressing NLRP3-mediated pyroptosis *via* P2X7/NF-κB/NLRP3 signaling pathway. *Front Pharmacol*. 2022;13:812362. https://doi.org/10.3389/fphar.2022.812362.
83 Wang R, Hu XL, Liu SM, et al. Kaempferol-3-*O*-sophoroside (PCS-1) contributes to modulation of depressive-like behaviour in C57BL/6J mice by activating AMPK. *Br J Pharmacol*. 2024;181(8):1182-1202. https://doi.org/10.1111/bph.16283.
84 Shi L, Yuan Z, Liu J, et al. Modified simiaowan prevents articular cartilage injury in experimental gouty arthritis by negative regulation of STAT3 pathway. *J Ethnopharmacol*. 2021;270:113825. https://doi.org/10.1016/j.

jep.2021.113825.
85 Zhang CYY, Zeng MJ, Zhou LP, et al. Baicalin exerts neuroprotective effects *via* inhibiting activation of GSK3β/NF-κB/NLRP3 signal pathway in a rat model of depression. *Int Immunopharmacol*. 2018;64:175-182. https://doi.org/10.1016/j.intimp.2018.09.001.
86 Li M, Yue GGL, Song LH, et al. Natural small molecule bigelovin suppresses orthotopic colorectal tumor growth and inhibits colorectal cancer metastasis *via* IL6/STAT3 pathway. *Biochem Pharmacol*. 2018;150:189-199. https://doi.org/10.1016/j.bcp.2018.02.017.
87 Wu XY, Tian F, Su MH, et al. Bf211, a derivative of bufalin, enhances the cytocidal effects in multiple myeloma cells by inhibiting the IL-6/JAK2/STAT3 pathway. *Int Immunopharmacol*. 2018;64:24-32. https://doi.org/10.1016/j.intimp.2018.08.016.
88 Chen XQ, Lv XY, Liu SJ. Baitouweng decoction alleviates dextran sulfate sodium-induced ulcerative colitis by regulating intestinal microbiota and the IL-6/STAT3 signaling pathway. *J Ethnopharmacol*. 2021;265:113357. https://doi.org/10.1016/j.jep.2020.113357.
89 Zhao Y, Luan H, Jiang H, et al. Gegen Qinlian Decoction relieved DSS-induced ulcerative colitis in mice by modulating Th17/Treg cell homeostasis *via* suppressing IL-6/JAK2/STAT3 signaling. *Phytomedicine*. 2021;84:153519. https://doi.org/10.1016/j.phymed.2021.153519.
90 Tong Y, Xu S, Huang L, et al. Obesity and insulin resistance: pathophysiology and treatment. *Drug Discov Today*. 2022;27(3):822-830. https://doi.org/10.1016/j.drudis.2021.11.001.
91 Wang Y, Xu Y, Zhang P, et al. Smiglaside a ameliorates LPS-induced acute lung injury by modulating macrophage polarization *via* AMPK-PPARγ pathway. *Biochem Pharmacol*. 2018;156:385-395. https://doi.org/10.1016/j.bcp.2018.09.002.
92 Xiao PT, Xie ZS, Kuang YJ, et al. Discovery of a potent FKBP38 agonist that ameliorates HFD-induced hyperlipidemia *via* mTOR/P70S6K/SREBPs pathway. *Acta Pharm Sin B*. 2021;11(11):3542-3552. https://doi.org/10.1016/j.apsb.2021.03.031.
93 Feng X, Yu W, Li X, et al. Apigenin, a modulator of PPARγ, attenuates HFD-induced NAFLD by regulating hepatocyte lipid metabolism and oxidative stress *via* Nrf2 activation. *Biochem Pharmacol*. 2017;136:136-149. https://doi.org/10.1016/j.bcp.2017.04.014.
94 Wang T, Huang X, Zhai K, et al. Integrating metabolomics and network pharmacology to investigate *Panax japonicus* prevents kidney injury in HFD /STZ-induced diabetic mice. *J Ethnopharmacol*. 2023;303:115893. https://doi.org/10.1016/j.jep.2022.115893.
95 Pôças ESC, Lopes DVS, da Silva AJM, et al. Structure–activity relationship of wedelolactone analogues: structural requirements for inhibition of Na^+, K^+-ATPase and binding to the central benzodiazepine receptor. *Biorg Med Chem*. 2006;14(23):7962-7966. https://doi.org/10.1016/j.bmc.2006.07.053.
96 Chen L, Jiang P, Li JS, et al. Periplocin promotes wound healing through the activation of Src/ERK and PI3K/Akt pathways mediated by Na/K-ATPase. *Phytomedicine*. 2019;57:72-83. https://doi.org/10.1016/j.phymed.2018.12.015.
97 Xu Y, Marck P, Huang M, et al. Biased effect of cardiotonic steroids on Na/K-ATPase-mediated signal transduction. *Mol Pharmacol*. 2021;99(3):217-225. https://doi.org/10.1124/molpharm.120.000101.
98 Pithayanukul P, Lapett B, Bavovada R, et al. Inhibition of proteolytic and hemorrhagic activities by ethyl acetate extract of *Eclipta prostrata*. Against Malayan pit viper venom. *Pharm Biol*. 2008;45(4):282-288. https://doi.org/10.1080/13880200701214805.
99 Wang Y, Xu Y, Xu X, et al. *Ginkgo biloba* extract ameliorates atherosclerosis *via* rebalancing gut flora and microbial metabolism. *Phytother Res*. 2022;36(6):2463-2480. https://doi.org/10.1002/ptr.7439.
100 Vinayagam R, Lee K, David E, et al. Facile green preparation of PLGA nanoparticles using wedelolactone: its cytotoxicity and antimicrobial activities. *Inorg Chem Commun*. 2021;129:108583. https://doi.org/10.1016/j.inoche.2021.108583.
101 Liu R, Liu XY, Li M, et al. Eurobusones A–D, four antibacterial formyl phloroglucinol meoterpenoids from *Eucalyptus robusta*. *Fitoterapia*. 2022;157:105131. https://doi.org/10.1016/j.fitote.2022.105131.
102 Kumar V, Sharma K, Ahmed B, et al. Deconvoluting the dual hypoglycemic effect of wedelolactone isolated from *Wedelia calendulacea*: investigation *via* experimental validation and molecular docking. *RSC Advances*. 2018;8(32):18180-18196. https://doi.org/10.1039/C7RA12568B.
103 Ding X, Zhao H, Qiao C. Icariin protects podocytes from NLRP3 activation by Sesn2-induced mitophagy through the Keap1-Nrf2/HO-1 axis in diabetic nephropathy. *Phytomedicine*. 2022;99:154005. https://doi.org/10.1016/j.phymed.2022.154005.
104 He H, Halseth TA, Mei L, et al. Nanodisc delivery of liver X receptor agonist for the treatment of diabetic nephropathy. *J Control Release*. 2022;348:1016-1027. https://doi.org/10.1016/j.jconrel.2022.06.029.
105 Su K, Yi B, Yao BQ, et al. Liraglutide attenuates renal tubular ectopic lipid deposition in rats with diabetic nephropathy by inhibiting lipid synthesis and promoting lipolysis. *Pharmacol Res*. 2020;156:104778. https://doi.org/10.1016/j.phrs.2020.104778.
106 Ramachandran V, Arokia VAM, David E, et al. Antidiabetic activity of gold nanoparticles synthesized using wedelolactone in RIN-5F cell line. *Antioxidants*. 2019;9(1):8. https://doi.org/10.3390/antiox9010008.
107 Chang S, Ruan WC, Xu YZ, et al. The natural product 4, 10-aromadendranediol induces neuritogenesis in neuronal cells *in vitro* through activation of the ERK pathway. *Acta Pharmacol Sin*. 2017;38(1):29-40. https://doi.org/10.1038/aps.2016.115.
108 Wu X, Li C, Chen L, et al. Protective effects of tauroursodeoxycholic acid on lipopolysaccharide-induced cognitive impairment and neurotoxicity in mice. *Int Immunopharmacol*. 2019;72:166-175. https://doi.org/10.1016/j.intimp.2019.03.065.
109 Wang L, Zhang S, Han J, et al. Activation of sting pathway contributed to cisplatin-induced cardiac dysfunction *via* promoting the activation of TNF-α-AP-1 signal pathway. *Front Pharmacol*. 2021;12:711238. https://doi.org/10.3389/fphar.2021.711238.
110 Maya S, Prakash T, Goli D. Effect of wedelolactone and gallic acid on quinolinic acid-induced neurotoxicity and impaired motor function: significance to sporadic amyotrophic lateral sclerosis. *Neurotoxicology*. 2018;68:1-12. https://doi.org/10.1016/j.neuro.2018.06.015.
111 Maya S, Prakash T, Goli D. Evaluation of neuroprotective effects of wedelolactone and gallic acid on aluminium-induced neurodegeneration: relevance to sporadic amyotrophic lateral sclerosis. *Eur J Pharmacol*. 2018;835:41-51. https://doi.org/10.1016/j.ejphar.2018.07.058.
112 Sharma S, Trivedi S, Pandey T, et al. Wedelolactone mitigates parkinsonism *via* alleviating oxidative stress and mitochondrial dysfunction through NRF2/skn-1. *Mol Neurobiol*. 2020;58(1):65-77. https://doi.org/10.1007/s12035-020-02080-4.
113 Hu J, Zhang L, Fu F, et al. Cardioprotective effect of ginsenoside Rb1 *via* regulating metabolomics profiling and AMP-activated protein kinase-dependent mitophagy. *J Ginseng Res*. 2022;46(2):255-265. https://doi.org/10.1016/j.jgr.2021.06.011.
114 Taleb A, Ahmad KA, Ihsan AU, et al. Antioxidant effects and mechanism of silymarin in oxidative stress induced cardiovascular diseases. *Biomed Pharmacother*. 2018;102:689-698. https://doi.org/10.1016/j.biopha.2018.03.140.
115 Wang A, Cai D, Zhang H, et al. Using herbal medicine to target the "microbiota-metabolism-immunity" axis as possible therapy for cardiovascular disease. *Pharmacol Res*. 2019;142:205-222. https://doi.org/10.1016/j.phrs.2019.02.018.
116 Sun J, Chen L, Jiang P, et al. Phenylethanoid glycosides of callicarpa kwangtungensis chun exert cardioprotective effect by weakening Na^+-K^+-ATPase/Src/erk1/2 pathway and inhibiting apoptosis mediated by oxidative stress and inflammation. *J Ethnopharmacol*. 2020;258:112881. https://doi.org/10.1016/j.jep.2020.112881.
117 Zhang XY, Lin W, Lei SY, et al. The anti-hyperlipidemic effects of *Poria cocos* (Schw.) Wolf extract: modulating cholesterol homeostasis in hepatocytes *via* PPARα pathway. *J Ethnopharmacol*. 2024;321:117532. https://doi.org/10.1016/j.jep.2023.117532.
118 Xia Y, Chen J, Cao Y, et al. Wedelolactone exhibits anti-fibrotic effects on human hepatic stellate cell line LX-2. *Eur J Pharmacol*. 2013;714(1-3):105-111. https://doi.org/10.1016/j.ejphar.2013.06.012.
119 Zeng GZ, Wang Z, Zhao LM, et al. NF-κB and JNK mediated apoptosis and G_0/G_1 arrest of HeLa cells induced by rubiarbonol G, an arborinane-type triterpenoid from *Rubia yunnanensis*. *J Ethnopharmacol*. 2018;220:220-227. https://doi.org/10.1016/j.jep.2017.10.026.
120 Zhang Q, Hu X, Hui F, et al. Ethanol extract and its dichloromethane fraction of *Alpinia oxyphylla* Miquel exhibited hepatoprotective effects against CCl_4-induced oxidative damage *in vitro* and *in vivo* with the involvement of Nrf2. *Biomed Pharmacother*. 2017;91:812-822. https://doi.org/10.1016/j.biopha.2017.04.131.
121 Lu Y, Ma J, Li P, et al. Ilexgenin A restrains CRTC2 in the cytoplasm to prevent srebp1 maturation *via* AMP kinase activation in the liver. *Br J Pharmacol*. 2022;179(5):958-978. https://doi.org/10.1111/bph.15369.
122 Honda S, Fukami T, Hirosawa K, et al. Differences in hydrolase activities in the liver and small intestine between marmosets and humans. *Drug Metab Dispos*. 2021;49(9):718-728. https://doi.org/10.1124/dmd.121.000513.
123 Lu Y, Hu D, Ma S, et al. Protective effect of wedelolactone against CCl_4-induced acute liver injury in mice. *Int Immunopharmacol*. 2016;34:44-52. https://doi.org/10.1016/j.intimp.2016.02.003.
124 Kang D, Shao Y, Zhu Z, et al. Systematically identifying the hepatoprotective ingredients of schisandra lignan extract from pharmacokinetic and pharmacodynamic perspectives. *Phytomedicine*. 2019;53:182-192. https://doi.org/10.1016/j.phymed.2018.09.010.
125 Zhou ZT, Deng LM, Hu LJ, et al. Hepatoprotective effects of ZLY16, a dual peroxisome proliferator-activated receptor α/δ agonist, in rodent model of nonalcoholic steatohepatitis. *Eur J Pharmacol*. 2020;882:173300. https://doi.org/10.1016/j.ejphar.2020.173300.
126 Wu J, Chen P, Ju L, et al. Corydalis saxicola bunting total alkaloids ameliorate diet-induced non-alcoholic steatohepatitis by regulating hepatic PI3K/Akt and TLR4/NF-κB pathways in mice. *Biomed Pharmacother*. 2022;151:113132. https://doi.org/10.1016/j.biopha.2022.113132.
127 Chen R, Zhang Y, Patel N, et al. CARD9 mediated MAPK/NF-κB signal pathway participates in the pathophysiological process of septic hepatitis: the role of tiliroside. *Int Immunopharmacol*. 2023;124:110275. https://doi.org/10.1016/j.intimp.2023.110275.
128 Li YQ, Chen Y, Fang JY, et al. Integrated network pharmacology and zebrafish model to investigate dual-effects components of cistanche tubulosa for treating both osteoporosis and alzheimer's disease. *J Ethnopharmacol*. 2020;254:112764. https://doi.org/10.1016/j.jep.2020.112764.
129 Dong P, Zhu D, Deng X, et al. Effect of hydroxyapatite nanoparticles and wedelolactone on osteoblastogenesis from bone marrow mesenchymal stem cells. *J Biomed Mater Res A*. 2018;107(1):145-153. https://doi.org/10.1002/jbm.a.36541.
130 Deng X, Tan S, Zhu D, et al. The combined effect of oleonuezhenide and wedelolactone on proliferation and osteoblastogenesis of bone marrow mesenchymal stem cells. *Phytomedicine*. 2019;65:153103. https://doi.org/10.1016/j.phymed.2019.153103.
131 Zheng ZG, Zhang X, Zhou YP, et al. Anhydroicaritin, a SREBPs inhibitor, inhibits RANKL-induced osteoclastic differentiation and improves diabetic osteoporosis in STZ-induced mice. *Eur J Pharmacol*. 2017;809:156-162. https://doi.org/10.1016/j.ejphar.2017.05.017.
132 Ju L, Hu P, Chen P, et al. Huoxuezhitong capsule ameliorates MIA-induced osteoarthritis of rats through suppressing PI3K/ Akt/ NF-κB pathway. *Biomed Pharmacother*. 2020;129:110471. https://doi.org/10.1016/j.biopha.2020.110471.
133 Ju LJ, Hu PP, Chen P, et al. *Corydalis saxicola* bunting total alkaloids attenuate walker 256-induced bone pain and osteoclastogenesis by suppressing RANKL-induced NF-κB and c-fos/NFATc1 pathways in rats. *Front Pharmacol*. 2021;11:609119. https://doi.org/10.3389/fphar.2020.609119.
134 Chen L, Li JS, Ke X, et al. The therapeutic effects of *Periploca forrestii* Schltr. stem extracts on collagen-induced arthritis by inhibiting the activation of

Src/NF-κB signaling pathway in rats. *J Ethnopharmacol*. 2017;202:12-19. https://doi.org/10.1016/j.jep.2017.03.005.
135 Jiang J, Xiao SC, Xu XM, et al. Isomeric flavonoid aglycones derived from Epimedii Folium exerted different intensities in anti-osteoporosis through OPG/RANKL protein targets. *Int Immunopharmacol*. 2018;62:277-286. https://doi.org/10.1016/j.intimp.2018.07.017.
136 Wang C, Song Y, Gu Z, et al. Wedelolactone enhances odontoblast differentiation by promoting Wnt/*β*-catenin signaling pathway and suppressing NF-κB signaling pathway. *Cell Reprogram*. 2018;20(4):236-244. https://doi.org/10.1089/cell.2018.0004.
137 Zhi H, Dai YD, Su L, et al. Thioacetamide-induced acute liver injury increases metformin plasma exposure by downregulating renal OCT2 and MATE1 expression and function. *Biomedicines*. 2023;11(12):3314. https://doi.org/10.3390/biomedicines11123314.
138 Liao XY, Deng QQ, Han L, et al. Leflunomide increased the renal exposure of acyclovir by inhibiting OAT1/3 and MRP2. *Acta Pharmacol Sin*. 2020;41(1):129-137. https://doi.org/10.1038/s41401-019-0283-z.
139 Yang Y, Zhang Z, Li P, et al. A whole-body physiologically based pharmacokinetic model characterizing interplay of octs and mates in intestine, liver and kidney to predict drug-drug interactions of metformin with perpetrators. *Pharmaceutics*. 2021;13(5):698. https://doi.org/10.3390/pharmaceutics13050698.
140 Vaziri ND. Roles of oxidative stress and antioxidant therapy in chronic kidney disease and hypertension. *Curr Opin Nephrol Hypertens*. 2004;13(1):93-99. https://doi.org/10.1097/00041552-200401000-00013.
141 Tian F, Wang Z, He J, et al. 4-Octyl itaconate protects against renal fibrosis *via* inhibiting TGF-β/Smad pathway, autophagy and reducing generation of reactive oxygen species. *Eur J Pharmacol*. 2020;873:172989. https://doi.org/10.1016/j.ejphar.2020.172989.
142 Li W, He W, Xia P, et al. Total extracts of *Abelmoschus manihot* L. attenuates adriamycin-induced renal tubule injury *via* suppression of ROS-ERK1/2-mediated NLRP3 inflammasome activation. *Front Pharmacol*. 2019;10:567. https://doi.org/10.3389/fphar.2019.00567.
143 Zhi D, Zhang M, Lin J, et al. Wedelolactone improves the renal injury induced by lipopolysaccharide in HK-2 cells by upregulation of protein tyrosine phosphatase non-receptor type 2. *J Int Med Res*. 2021;49(5):3000605211012665. https://doi.org/10.1177/03000605211012665.
144 Wu X, Bian D, Dou Y, et al. Asiaticoside hinders the invasive growth of keloid fibroblasts through inhibition of the GDF-9/MAPK/Smad pathway. *J Biochem Mol Toxicol*. 2017;31(8):e21922. https://doi.org/10.1002/jbt.21922.
145 Shi W, Hao J, Wu Y, et al. Protective effects of heterophyllin B against bleomycin-induced pulmonary fibrosis in mice *via* AMPK activation. *Eur J Pharmacol*. 2022;921:174825. https://doi.org/10.1016/j.ejphar.2022.174825.
146 Tao L, Cao F, Xu G, et al. Mogroside IIIE attenuates LPS-induced acute lung injury in mice partly through regulation of the TLR4/MAPK/NF-κB axis *via* AMPK activation. *Phytother Res*. 2017;31(7):1097-1106. https://doi.org/10.1002/ptr.5833.
147 Yang T, Liu XL, Zhou Y, et al. Sanpian decoction ameliorates cerebral ischemia-reperfusion injury by regulating SIRT1/ERK/HIF-1α pathway through *in silico* analysis and experimental validation. *J Ethnopharmacol*. 2024;318:116898. https://doi.org/10.1016/j.jep.2023.116898.
148 Khan GJ, Gao Y, Gu M, et al. TGF-β1 causes EMT by regulating *N*-Acetyl glucosaminyl transferases *via* downregulation of non muscle myosin II-A through JNK/P38/PI3K pathway in lung cancer. *Curr Cancer Drug Targets*. 2018;18(2):209-219. https://doi.org/10.2174/1568009617666170807120304.
149 Guo JS, Fang YS, Jiang FX, et al. Neohesperidin inhibits TGF-β1/Smad3 signaling and alleviates bleomycin-induced pulmonary fibrosis in mice. *Eur J Pharmacol*. 2019;864:172712. https://doi.org/10.1016/j.ejphar.2019.172712.
150 Guan C, Qiao S, Lv Q, et al. Orally administered berberine ameliorates bleomycin-induced pulmonary fibrosis in mice through promoting activation of PPAR-γ and subsequent expression of HGF in colons. *Toxicol Appl Pharmacol*. 2018;343:1-15. https://doi.org/10.1016/j.taap.2018.02.001.
151 Li XY, Ding Z, Wu ZX, et al. Targeting the TGF-β signaling pathway for fibrosis therapy: a patent review (2015-2020). *Expert Opin Ther Pat*. 2021;31(8):723-743. https://doi.org/10.1080/13543776.2021.1896705.
152 Yu HL, Li JY, Hu XL, et al. Protective effects of cynaroside on oxidative stress in retinal pigment epithelial cells. *J Biochem Mol Toxicol*. 2019;33(8):e22352. https://doi.org/10.1002/jbt.22352.
153 Xu J, Zhang M, Zhang X, et al. Contribution of hepatic retinaldehyde dehydrogenase induction to impairment of glucose metabolism by high-fat-diet feeding in C57BL/6J mice. *Basic Clin Pharmacol Toxicol*. 2018;123(5):539-548. https://doi.org/10.1111/bcpt.13039.
154 He T, Shang J, Gao C, et al. A novel SIRT6 activator ameliorates neuroinflammation and ischemic brain injury *via* EZH2/FOXC1 axis. *Acta Pharm Sin B*. 2021;11(3):708-726. https://doi.org/10.1016/j.apsb.2020.11.002.
155 Li X, Wang T, Liu J, et al. Effect and mechanism of wedelolactone as antioxidant-coumestan on OH-treated mesenchymal stem cells. *Arabian J Chem*. 2020;13(1):184-192. https://doi.org/10.1016/j.arabjc.2017.03.008.
156 Xin P, Xu X, Deng C, et al. The role of JAK/STAT signaling pathway and its inhibitors in diseases. *Int Immunopharmacol*. 2020;80:106210. https://doi.org/10.1016/j.intimp.2020.106210.
157 Zhao Q, Liu YC, Wang T, et al. MiR-375 inhibits the sternness of breast cancer cells by blocking the JAK2/STAT3 signaling. *Eur J Pharmacol*. 2020;884:173359. https://doi.org/10.1016/j.ejphar.2020.173359.
158 Wang R, Hu X, Wang J, et al. Proanthocyanidin A1 promotes the production of platelets to ameliorate chemotherapy-induced thrombocytopenia through activating JAK2/STAT3 pathway. *Phytomedicine*. 2022;95:153880. https://doi.org/10.1016/j.phymed.2021.153880.
159 Zhao L, Han S, Chai C. Huangkui Capsule alleviates doxorubicin-induced proteinuria *via* protecting against podocyte damage and inhibiting JAK/STAT signaling. *J Ethnopharmacol*. 2023;306:116150. https://doi.org/10.1016/j.jep.2023.116150.
160 Upadhyay K, Gupta NK, Dixit VK. Development and characterization of phyto-vesicles of wedelolactone for hepatoprotective activity. *Drug Dev Ind Pharm*. 2012;38(9):1152-1158. https://doi.org/10.3109/03639045.2011.643892.
161 Du G, Fu L, Jia J, et al. Validated UPLC-MS/MS method for quantification of seven compounds in rat plasma and tissues: application to pharmacokinetic and tissue distribution studies in rats after oral administration of extract of *Eclipta prostrata* L.. *Biomed Chromatogr*. 2018;32(6):e4191. https://doi.org/10.1002/bmc.4191.
162 Jiang S, Zhong YL, Qiao HW, et al. UPLC-MS/MS method for the simultaneous quantification of caffeine and illicit psychoactive drugs in hair using a single-step high-speed grinding extraction: insights into a cut-off value for caffeine abuse. *J Pharmaceut Biomed*. 2022;209:114489. https://doi.org/10.1016/j.jpba.2021.114489.
163 Wang Y, Li Q, Dai Y, et al. Development of a LC-MS/MS method to investigate the interference of pharmacokinetics of the main constituents in *Saxifraga stolonifera*: involvement of drug metabolism enzymes. *J Pharm Biomed Anal*. 2018;148:128-135. https://doi.org/10.1016/j.jpba.2017.08.019.
164 Yang W, Sabi-Mouka EMB, Wang L, et al. Determination of tranilast in bio-samples by LC-MS/MS: application to a pharmacokinetic and brain tissue distribution study in rats. *J Pharm Biomed Anal*. 2018;147:479-484. https://doi.org/10.1016/j.jpba.2017.06.047.
165 Yang Y, Lian Y, Zhong P, et al. Characterization and quantitative analysis of related substances in coenzyme A by HPLC and LC-MS/MS. *J Pharm Biomed Anal*. 2018;150:220-232. https://doi.org/10.1016/j.jpba.2017.11.051.
166 Wang Y, Liu YH, Sha YT, et al. Development and validation of a chiral UPLC-MS/MS method for quantifying *S*-oxiracetam and *R*-oxiracetam in human plasma, urine and feces: application to a phase-I clinical pharmacokinetic study. *J Pharm Biomed Anal*. 2024;239:115881. https://doi.org/10.1016/j.jpba.2023.115881.
167 Wang WQ, Chen C, Luo J, et al. Metabolism investigation of the peptide-drug conjugate LN005 in rats using UHPLC-HRMS. *J Pharm Biomed Anal*. 2024;238:115860. https://doi.org/10.1016/j.jpba.2023.115860.
168 Yang J, Lin J, Wang A, et al. Study on the effect of calibration standards prepared with different matrix on the accuracy of bile acid quantification using LC-MS/MS. *J Pharm Biomed Anal*. 2024;237:115785. https://doi.org/10.1016/j.jpba.2023.115785.
169 Cheruvu HS, Yadav NK, Valicherla GR, et al. LC-MS/MS method for the simultaneous quantification of luteolin, wedelolactone and apigenin in mice plasma using hansen solubility parameters for liquid-liquid extraction: application to pharmacokinetics of *Eclipta alba* chloroform fraction. *J Chromatogr B*. 2018;1081-1082:76-86. https://doi.org/10.1016/j.jchromb.2018.01.035.
170 Chen Q, Wu X, Gao X, et al. Development and validation of an ultra-performance liquid chromatography method for the determination of wedelolactone in rat plasma and its application in a pharmacokinetic study. *Molecules*. 2019;24(4):762. https://doi.org/10.3390/molecules24040762.
171 Alolga RN, Chavez MASC, Muyaba M. Untargeted UPLC-Q/TOF-MS-based metabolomics and inductively coupled plasma optical emission spectroscopic analysis reveal differences in the quality of ginger from two provinces in Zambia. *J Pharm Pharmacol*. 2018;70(9):1262-1271. https://doi.org/10.1111/jphp.12959.
172 Zhu BJ, Cao HT, Sun LM, et al. Metabolomics-based mechanisms exploration of Huang-Lian Jie-Du Decoction on cerebral ischemia *via* UPLC-Q-TOF/MS analysis on rat serum. *J Ethnopharmacol*. 2018;216:147-156. https://doi.org/10.1016/j.jep.2018.01.015.
173 Xu ZL, Wang BE, Zhang LT, et al. UPLC-MS/MS assay for quantification of wedelolactone and demethylwedelolactone in rat plasma and the application to a preclinical pharmacokinetic study. *Comb Chem High Throughput Screen*. 2022;25(8):1271-1277. https://doi.org/10.2174/1386207324666210520093517.
174 Li L, Huang XJ, Peng JL, et al. Wedelolactone metabolism in rats through regioselective glucuronidation catalyzed by uridine diphosphate-glucuronosyltransferases 1As (UGT1As). *Phytomedicine*. 2016;23(4):340-349. https://doi.org/10.1016/j.phymed.2016.01.007.
175 Feng L, Li ZY, Wang L, et al. Wedelolactone-loaded micelles ameliorate doxorubicin-induced oxidative injury in podocytes by improving permeability and bioavailability. *Front Bioeng Biotechnol*. 2019;7:333. https://doi.org/10.3389/fbioe.2019.00333.
176 Zhang X, Li N, Liu Y, et al. On-demand drug release of ICG-liposomal wedelolactone combined photothermal therapy for tumor. *Nanomedicine*. 2016;12(7):2019-2029. https://doi.org/10.1016/j.nano.2016.05.013.
177 Zhang X, Liu Y, Luo L, et al. A chemo-photothermal synergetic antitumor drug delivery system: gold nanoshell coated wedelolactone liposome. *Mater Sci Eng C Mater Biol Appl*. 2019;101:505-512. https://doi.org/10.1016/j.msec.2019.04.006.